Review 1 (reviewer comments in italic)

This is a very nice piece of work!
The authors present some important methodological advances. The use of the adjoint method to calculate the grounding-line flux is very nice, and of course far better than the approach used in Reese et al (full disclosure, I was one of the authors of the paper, and it should have been my job to implement the adjoint approach myself for that work, but I was too busy with other things. . .So I'm very glad that someone has now done what I myself should have done some time ago.)

We appreciate the general endorsement of the work and the helpful suggestions below, which we have used to clarify and improve the paper.

I like the three research questions and I think the authors provide very satisfying answers to all of them in the paper. I wonder if the research question (1) could not be formulated a bit better? Maybe: How do changes in ice-flux across grounding line relate to estimates of ice-shelf buttressing evaluated at locations within the ice-shelf?

Thanks for the suggestion. We have changed the initial version of this question "Do local evaluations of ice shelf buttressing reflect how local perturbations in ice shelf thickness impact grounding line flux?" to "How do changes in ice-flux across the grounding line relate to local estimates of ice-shelf buttressing evaluated on the ice-shelf?"

Must confess that I have never myself fully understood the usefulness of quantifying buttressing at some location within an ice shelf. What makes sense to me is to quantify the grounding-line buttressing provided by an ice shelf, and the changes in GL buttressing and GL ice flux as a function of thickness-perturbation across the ice shelf. I guess in some way the authors also address this issue when they conclude that the buttressing at a given location within an ice shelf depend critically on the normal direction chosen. (Possibly it might be better just to look at, in a general sense, how stresses within an ice shelf differ from the unconfined case, but again this will depend on the particular question being addressed.)

The authors investigate the possibly that perturbations in ground-line flux due to local changes in ice-shelf thickness, are linearly related to ice-shelf buttressing values calculated at those same locations within the ice shelf. This is an important point that needs to be investigated, and I guess it could be argued that Fuerst et al implicitly assumed this to be the case. (As mentioned above, I personally have never understood why one would expect there to be a simple correlation between these two quantities, except possibly in some general qualitative sense.) But this has been implicitly assumed in some previous work, and the authors are the first ones to actually look into this in any detail. They provide a detailed but arguably also a too long and somewhat confusing answer, but essentially I think they conclude that there is not simple relationship between these two. If I have correctly understood their conclusion, I would recommend stating more clearly this key finding and basically just write that there is no

theoretical reason to expect GLF to scale in a simple way with buttressing numbers evaluated at a given location within the ice shelf, and that the numerical experiments show that no such simple relationship exists for the cases considered.

As suggested by the reviewer, throughout the revised manuscript we have attempted to (1) clarify that this is one of our primary conclusions, (2) more clearly tie together the various sections of the paper that need to be understood to support this conclusion, and (3) justify this conclusion based on the results and discussion presented in the paper.

I had some difficulties following the discussion in 4.3.2. Not sure if this is really relevant, but a reduction in ice thickness change at any location within an ice shelf will generally have two opposing effects on ice-shelf flow: 1) the spreading rate goes down and with it the speed further downstream 2) buttressing (as measured along the grounding lines upstream) will generally decrease and therefore speed increase. So there are two exactly opposing effects involved. Usually, reduction in ice-shelf thickness leads to an increase speed close to the grounding line, and decrease further downstream (provided the ice-shelf is long enough for the integrated effect of ice-shelf thinning to outweigh the effect on increased GL speed.)

The manuscript is still in a bit rough state. In fact, I find it to be in an unusually rough state compared to a typical TC submission. There are number of footnotes, and these seem to be mostly some comments aimed at the authors themselves.

This needs to be sorted out and the presentation of the material needs to be sharpened up a bit (what are 'distal changes'?).

We have largely rewritten all of section 4.3 and attempted to clarify the main points therein and better connect them to the preceding and following sections, in order to better support the main findings of the paper. We also have removed most of the footnotes, either deleting them or incorporating them directly into the main text.

The figures are also some of rather poor quality. I guess most TC readers will know where the Larsen C is, but it might nevertheless be good to have some map showing the location of Larsen C.

A location figure for Larsen C has been added to Figure 1. We have also added several other new figures (mainly to the SI, in response to other reviewers). In general, the majority of figures and their captions have been updated and improved.

It's a bit unusual to use curly brackets around a tensor as done in Eq, (11).

The brackets in Eq. (11) have been changed to parentheses.

I missed an exact definition of the grounding-line flux and the GLF used in the adjoint method. Is it a line integral over all the grounding lines?

The reviewer is correct. We have added a new section up front (2.1.1) to clarify how the grounding line flux is calculated (along with additional discussion relating to the adjoint approach in Appendix C).

How is the grounding-line defined at a local element level? Do you use the edges of the grounded elements, or do you cut through elements based on the flotation/grounding mask? If so, how do you interpolate velocities and ice thickness from the nodal points?

The location of the grounding line in the model is defined at sub-grid resolution (i.e., “cut through”) using a floating vs. grounded mask. Velocities and thickness are discretized as nodal finite element fields and are evaluated on the grounding line. This is now explained in detail in the new section 2.1.1.

Line 193-194: Not sure if I actually showed this. At least I don’t think I used the concept of ‘group velocity’ in this context.

We have removed this discussion in the updated version of the manuscript so this is no longer relevant.

I would generally have recommended a minor revision to such an excellent work. But the presentation is still too poor, and for that reason I suggest a revision following a re-review.

The manuscript has been significantly revised since the initial submission and we believe that all of the reviewers concerns are adequately addressed.

Review 2 (reviewer comments in italic)

In this study, Zhang et al. present a detailed and thorough analysis of the relation between local ice-shelf buttressing numbers, how they are affected by local perturbations and how they relate to the flux response at the grounding line induced by such a local perturbation. They find that correlations between the flux response (see Reese et al., 2018) and the local buttressing numbers (see Fürst et al., 2016) can be found in very specific cases, but break down for more complicated geometries and when considering regions close to the grounding line. In a second step, they show how the adjoint method could be used to assess the sensitivity of grounding line flux to local perturbations which is shown to be consistent with the computationally more intense perturbation approach (except at the grounding line).

This study presents very interesting results that will help to advance the understanding of ice-shelf buttressing significantly. However, I think that some points should be addressed before it could be published.

We thank the reviewer for all of the helpful comments below.

Major comments

Your manuscript would be much easier to read if the central questions and related main findings of your paper were formulated more clearly. This shows for example in your abstract, where you state that you search for causal connections between sub-shelf melting, buttressing and grounding line flux. However, there is no clear answer to that, you rather switch to presenting an alterative method to calculate the grounding line flux sensitivity in the second part of the abstract. This is also reflected, for example, in the formulation of the research questions on page 2, line 47-52.

We have modified the abstract to remove the focus on understanding the causal connections between melt perturbations, buttressing, and grounding line flux. The research questions in the introduction have also been slightly modified (also in response to reviewer no. 1). As discussed further below, we have also significantly updated and improved the content and writing relative to our initial submission.

Section: 4.5: You state that the differences between the adjoint approach and the perturbation approach near the grounding line arise from 'nonlinearities' - more clarification is required at this point. In particular, Figures 13 and 14 show that the adjoint-sensitivites are negative along the grounding line, while Figure 15 indicates in general positive sensitivities in the perturbation approach. I think that the treatment of the grounding line in the sensitivity assessment could be key in explaining these differences.

We interpret the large nonlinearities close to the grounding line as a consequence of 1) relatively large thickness gradients and the rapid transition from vertical-shear-dominated to

membrane-stress-dominated flow close to the grounding line, and 2) the changes of grounding line position and local geometry due to the change of thickness in the cells adjacent to the grounding line. This is now more clearly stated in the manuscript.

In terms of the difference between Figs. 13, 14 versus Fig. 15 (11, 12, and 13 in the revised version), the analysis in current Fig. 13 focuses on a small fraction of the total number of perturbation points -- those near the grounding line -- whereas current Figs. 11, 12 include those same points plus many more points (all in the case of MISMIP+) on the ice shelf proper. Thus, there are relatively more negative values obvious in current Fig. 13.

So please explain (1) how you specify the grounding line position in your experiments / model and how grounding line flux is calculated (can the grounding line move in your perturbation experiments?),

We have added a new section, 2.1.1, in which we detail the computation of the GL and the GLF. We also note that a perturbation to the ice thickness at a (triangular) grid cell intersecting the GL will affect both the GL position and length (because the thickness affects the flotation condition, which in turn can affect the position of the GL).

(2) if these differences arise only for cells directly adjacent to the grounding line, and

We observe negative sensitivities only for cells intersecting the grounding line. This can also happen for the perturbation-based sensitivity approach, as shown in Figure 2a (for the Larsen C case, the perturbation points are randomly chosen and we are not reporting results for all of the points at the grounding line). Differences between the adjoint-based and the perturbation-based sensitivities are more pronounced near the grounding line and become smaller far from the grounding line, as shown in revised Figure 13 of the paper.

(3) how this is reflected in the adjoint method. In addition, issues might arise due to the discretization. Perturbations in the ice shelf should theoretically not be able to change the ice thickness at the grounding line or the surface slope upstream, but they do so in numerical models, so it could be argued that including these regions is anyway problematic

The reviewer is correct that perturbations on the ice shelf proper do not change the thickness or slope of the ice at the grounding line while they do in the case where a grid cell being perturbed also intersects with the grounding line (as now explained more carefully in section 2.1.1). For this reason we argue that one should refrain from including cells that intersect the grounding line when performing similar sensitivity analysis (when using either the adjoint- or perturbation-based approach). Further, one should also refine the mesh near the GL to get more accurate sensitivities near the GL. This is now stressed more clearly in section 4.5.

The adjoint method also accounts for possible changes in the GL position/length due to (infinitesimal) changes in the ice thickness at triangular grid cells intersecting the GL. This is now explained in more detail in (new) section 2.1.2 and Appendix C after equation C1.

We further note that, in the numerical model, the thickness on the ice shelf and along the grounding line does not change *prognostically.*

Title: In the manuscript you are not so much analysing the sensitivity of grounding line flux to perturbations itself, but you are rather (1) trying to relate the concept of buttressing numbers to the concept of locally-induced grounding line flux changes and (2) showing that the adjoint method is consistent with the perturbation approach. So I would suggest to reformulate your title to reflect the content better, maybe something in the direction of 'On the complicated relation between local ice-shelf buttressing and induced grounding line flux changes', 'Are there causal connections between local ice-shelf buttressing and locally-induced grounding line flux changes?' or 'Adjoint-based sensitivity of grounding line flux to sub-shelf melting...'

We appreciate the reviewer's suggestion. However, we have decided to keep the original title as we feel that it clearly encompasses and describes our efforts and the main focus of the paper.

page 1, line 7: I'm not sure if this is the correct argument to debunk a correlation between grounding line flux changes and local buttressing numbers. If the ice shelf is locally perturbed and buttressing at the grounding line is reduced, this speeds up ice flow at the grounding line up to the perturbation location. However, the perturbation will reduce the spreading rate and hence tends to reduce velocities at and downstream of the perturbation location. This shows in your figure 7 where velocities increase up to the perturbation location and decrease downstream of it, which is then reflected in a local reduction in longitudinal stresses. This is then interpreted as an increase in the local buttressing number based on, e.g., the flow direction. From this point of view, a reduction in buttressing at the grounding line can consistently be related to an increase in the local buttressing number. Your point here is supported by the fact that you cannot find correlations once you include regions close to the grounding line or you analyse Larsen C. Don't get me wrong, I think that it is a very important point to make that local perturbations increase locally measured buttressing numbers, as I do not think that many people are aware of that (I was not).

In general, the reviewer seems to be largely agreeing with the interpretation and conclusions we present in our paper. That is, that a local *increase* in buttressing number following perturbations is paradoxical with respect to the overall *decrease* in buttressing experienced by the broader ice shelf (leading to an *increase* in ice flux across the grounding line). Further, as we discuss in more detail in our revised manuscript (specifically, in sections 4.3.1 and 4.3.2), the local (at the perturbation location) change in buttressing is not always consistent and is often in opposition to the broader response immediately neighboring it. The reviewer may be proposing that the increase in buttressing number in the local area around a perturbation is a consistent diagnostic that could be used as a proxy for overall increases in grounding line flux. While this may be the

case for specific domains and perturbations, we are not comfortable making such a general statement here based on the analysis conducted.

page 1, line 20 and other: please check your references, e.g., Schoof (2012) does not use idealized modelling and Asay-Davis et al. (2016) do not include experiments showing MISI, also Royston and Gudmundsson (2016) analyse diagnostic responses to ice-shelf collapse.

We have changed the Schoof (2012) reference to the more appropriate Schoof (2007) reference. The Asay-Davis et al. (2016) reference was meant to be a placeholder for the MISMIP+ paper (which at the time of this submission, had not yet been submitted). We have updated it to the correct reference for the MISMIP+ experiments (Cornford et al. 2020).

page 2, line 43: 'diagnostic, forward experiments'

Changed.

page 4, line 86: you could add a subsection 'Initial configuration' here to improve readability.

Changed as suggested. A new "Model configuration" subsection (2.2) has been added.

page 5, line 120: You need to multiply Nrp with a time interval (e.g., one year if your flux is given in units per year) to get a dimensionless number.

In Reese et al. (2018), it is implicit that the time period of interest is one year (according to personal communications). Therefore, P should have units of m^3, which are the same units as R. We have explicitly stated that the units of R and P are both in m^3 (in which case their ratio is non-dimensional).

page 5, line 120: Do you exclude changes in grounding lines of ice rises in the Larsen C domain?

For the Larsen C domain, the grounding lines around ice rises are treated in the same way as the "primary" grounding line. Therefore, the cells close to ice rises will also be removed when we pick cells for analyzing based on the distance to the grounding line. We have added an explicit statement about the treatment of ice rises to section 2.1.1.

page 5, line 121: you could add a subsection 'Local buttressing number' here to improve readability.

Since this section is already fairly short, and to avoid breaking up the paper into too many short sections, we've opted to keep the discussion of the local buttressing number in with the discussion of the flux response number (and the perturbation experiments in general).

Figure 2: labels for the colorbars are missing and it would be easier to understand your message if you added the normal directions in the panels (also in Figure 3 and others).

We have added colorbar titles and also labels for the choice of buttressing-number normal direction to Figs. 2, 3 and 4.

page 7, line 156: Why 12km? Does the relation already improve if you remove only cells that are directly linked to the grounding line?

We have substantially revised this portion of the paper because we discovered a new metric that can be used for "removing" these areas from consideration (based largely on whether or not the region is experiencing significant shear and/or close to the grounding line). This is discussed in the update section 4.1 (and new Figure S2).

Figure 4: Please add p-values for your correlation statistics.

The p values, relative to the null hypothesis that N_{rp} is independent of N_b, are 1.23e-59 for $\mathbf{n}_{p1}$, 1.57e-09 for $\mathbf{n}_{p2}$ and 5.20e-31 for $\mathbf{n}_{flow}$. However, we think that it would be misleading to report these exceedingly small p-values in the paper. Here, we are trying to assess whether N_{rp} and N_b are linearly related and for this reason we are using linear regression to compute the fitting line and the correlation coefficient, to quantify the discrepancy from that line. We are not interested in ascribing a statistical interpretation to this line fit (which would then need to be explained / defended). For these reasons, we argue against including p-values in the paper.

page 8, line 174, isn't this a contradiction to your statement in p7., line 58?

We have changed Line 158 (now Line 198; end of section 4.2) to "... we find that buttressing in this direction is not useful for predicting changes in GLF; compared to $N_b(\mathbf{n}_{p2})$, $N_b(\mathbf{n}_{p1})$ and $N_b(\mathbf{n}_f)$ both show a better correlation with changes in GLF via local, sub-ice shelf melt perturbations.", for consistency with old line 174.

page 11, line 195, maybe better state that the thickness gradients magnitude increases / decreases, since this is the relevant quantity to drive ice flow.

Because the change in thickness gradient *magnitude* doesn't allow for any information regarding how the change in ice thickness impacts the *direction* of the ice flow, we prefer to keep the wording here as is. This is important because with no information regarding the sign of the gradient change, it's not immediately obvious if the change in thickness gradient should lead to an increase or a decrease in the local ice velocity.

page 11, line 204: I do not understand your sentence in brackets, please clarify.

This section has been completely re-written.

Figure 8: why do you analyse buttressing changes in neighboring cells and not in the cell itself? This should not make a difference, given Fig. 7 etc, or do I miss some argument here?

In 4.3.1 and 4.3.2 we now discuss in detail the buttressing changes both at the perturbation location and in the immediately surrounding neighborhood.

page 12, line 218: you could add that this negative correlation is in line with the general understanding of how buttressing reduction affects ice flow.

We have revised this sentence to state this more explicitly (around line 266 in the revised manuscript).

Section 4.3.2.: when calculating buttressing at the grounding line, you have an additional direction that emerges naturally, which is the grounding line normal as used in Gudmundsson (2013). In fact, since the boundary condition at the calving front is formulated in terms of the calving front normal, this is the only direction that guarantees that you get a value of 1 if and only if you do not have any buttressing at the corresponding grounding line location. It is worth checking, how using that normal affects your findings.

We have updated this figure and the discussion around it, including (as suggested) the addition of a subplot showing the value of Eq. 14 when changes in buttressing are calculated in the direction normal to the grounding line (of Fig. 8a).

page 13, line 235: I do not understand your statement here as there is a difference between the first principal component along the grounding line and within the ice shelf?

This statement has been removed.

page 14, line 245: you state that you test experiments with and without perturbing elements that are crossed by the grounding line, but you never refer to these experiments again.

This section has been entirely revised. Updated versions of the figures (and the related discussion) from the original version are now included in the SI. With respect to this comment, we do not include cells that cross the grounding line but rather grid cells that are *close to the grounding line* but still on the ice shelf. These experiments are discussed in more detail in the following two paragraphs. Note that we have also edited this sentence to try to clarify its meaning.

page 15, line 266: It might be worth checking the flow and normal directions as well (similar to Figure S8 for the p1-direction).

The relevant figures are now all contained by Fig. S6 and the related discussion is also in the SI. Note that in those figures, we show correlations for all directions (i.e., 180 degrees around the p1 direction).

page 17, line 300: I suppose that you repeat the perturbations for the different thicknesses?

Correct. The experiments are repeated with different sized thickness perturbations. For clarity, we've added "the only change being the magnitude of the applied perturbation" in Line 329.

page 17, line 314: you refer here to the other methods discussed in the previous sections, i.e., the local buttressing numbers etc?

Correct. We've added a clarifying statement "Two previous approaches for assessing GLF sensitivity to changes in ice shelf buttressing – the flux response number (N_{rp})and the buttressing number (N_b)..." to this effect (line 357).

Review 3 (reviewer comments in italic)

Summary

In this manuscript, the author employ a new state-of-the-art ice-flow model and assess the utility of various buttressing metrics for inferring grounding line response to distant ice-shelf thinning. For this purpose, they reconcile two former studies that introduce metrics for the local ice-shelf buttressing and the integrated flux response along the grounding line (GL). For local thinning perturbations, the authors show that for relevant parts of an ice shelf (away from the GL and unconfined parts of the ice-shelf), there is a positive correlation between the two metrics. Highest values are found when the buttressing metrics is computed along the first principal stress direction (p1). Yet, buttressing values increase in the vicinity of the thinning perturbations, which seems counter-intuitive with respect to the concurrent increase in the grounding line flux (GLF). This finding makes changes in ice-shelf buttressing utterly difficult to interpret. In a final step, an adjoint-based GLF sensitivity is computed, which shows comparability to results from a large ensemble of forward evaluations. This sensitivity measure has the potential to be very useful in delineating ice-shelf areas relevant for restraining present outlet-glacier discharge.

In order to avoid possible misunderstandings, we point out that we do not conduct any forward model (i.e., prognostic) evaluations here. All experiments are strictly diagnostic in nature. We have stated this clearly in the revised manuscript.

I gladly admit that I was very excited about this study because the authors present a computationally efficient adjoint-based method to compute GLF sensitivities that gives identical results as a cumbersome diagnostic perturbation ensemble. Initially, they also convinced me about the limited utility of changes in the buttressing index. Yet after plunging into the review, I strongly contest this judgment because the underlying analysis seems somewhat biased (see below) and I urge the authors to moderate their assessment. The authors themselves show that the buttressing index along the p1-direction is actually very informative in terms of GLF sensitivity. This is a very important conclusion, which will be appreciated by modellers that cannot compute this adjoint-based sensitivity. Moreover, I have identified a potential error in the index calculation, which might have severe implications.

We were also initially similarly excited by the possibility of a computationally inexpensive and easily calculated metric for use in assessing the impact of local ice shelf thickness changes on changes in grounding line flux (i.e., a way to obtain the information from the Reese et al. calculations but with less effort). Indeed, this was an initial goal of our research, along with providing some physical basis for better understanding and justifying the apparent correlations between local measures of ice shelf buttressing and changes in grounding line flux.

In the end, however, we concluded that we cannot in good faith make a recommendation for using these apparent correlations. First, we've found it difficult to provide a clear explanation for their existence (i.e., the physical mechanisms connecting them). Second, we've found and

demonstrated clear contradictions between changes in buttressing on the shelf, in the vicinity of perturbations, and changes in integrated buttressing and grounding line flux, which are contrary to our understanding for how ice shelf buttressing works. Most important, however, is that even for simple or idealized ice shelf geometries, numerous data points near the grounding line -- the region that is most sensitive to perturbations -- must be removed for strong correlations to emerge. For a realistic ice shelf, only a small number of points near the center of the ice shelf remain useful at demonstrating the correlation. Lastly, as we show in a newly added Supplemental Table, there are many other physical quantities that correlate with changes in grounding line flux, some of which may simply be fortuitous or spurious (and, as with the buttressing number, we find that these same correlations become much weaker and less convincing when applied to realistic domains). Thus, while we appreciate the reviewer's comments, we argue that it is not within the goals or scope of the current work to come up with additional reasons to further justify the application of these easy-to-calculate metrics.

The potential error the reviewer alludes to is the swap of panels b and d in Figure 2. This is, however, an isolated mistake with no implications regarding the analysis conducted in the rest of the paper (as noted further below).

In summary, I remain very positive about this manuscript and I recommend that the editor should continue to consider it for publication in The Cryosphere after my concerns have been alleviated. This will require a major revision during which a fundamental change in the manuscript structure might be necessary.

We appreciate the reviewer's careful attention to our manuscript and, as detailed below, address as many of their concerns as we can without changing the fundamental interpretation of our results. We also note that many sections of the paper have been significantly revised relative to the initial submission, including additional analysis, arguments, and changes in presentation.

Erroneous calculation: From a vertically integrated perspective, the normal stress Tnn which is computed in the various directions should be maximal and minimal for the first (p1) and second (p2) principal stress directions, respectively. This implies that the buttressing is minimal in p1 and maximal in p2 direction (you show this nicely in Figure S1 yourself). In Figure 2, you show the buttressing values for the MISMIP+ setup in various directions. While the p2-values appear maximal, the p1 values seem larger than the values computed in flow direction. This cannot be correct. I suspect that you confused panels b) and c). If not, this comment might have severe implications. Please verify.

We appreciate the reviewer's pointing this out. The panel swap mentioned in Fig. 2 was definitely a mistake, which we have now corrected. The related buttressing number calculations, however, were / are correct and unaffected by this. Consequently, the mistake in this figure was isolated and did not / does not propagate to any of the discussion or conclusions in the rest of the paper.

Inconsistent and biased analysis: I certainly appreciate how carefully you have structured the analysis in this manuscript. You clearly state a correlation between the GLF response and the buttressing index in dynamically relevant areas (cf., Sect. 4.2, Fig.4). Thereafter, you show that buttressing changes in the vicinity of the thinning perturbations exhibit a counterintuitive behaviour which is difficult to interpret. Yet, this difficulty seems to have entirely undermined your confidence in the interpretability of this measure. In the abstract, you even condemn the correlation between the GLF and the local buttressing measures as remaining '[...] elusive from a physical perspective'.

This judgment is evoked throughout your manuscript and I somehow feel that I have to take up the cudgels for this metric. First, you show yourself that there can be good correlation (Figs. 4,5,11b). The more I tried to understand the details of your analysis, I have more and more doubts about its robustness. First doubts arose when I read through Sect. 4.3.1. You start by discussing non-local speed-up in the vicinity of the perturbed area (but excluding the centre). Thereafter, you focus on the local-scale buttressing changes within the perturbed area. This seemed inconsistent and this choice biases and discredits the buttressing change measure.

As noted above, we do eventually conclude that the correlation between local buttressing number and grounding line flux should not be applied in a 'predictive' sense (i.e., to diagnose the difficulty to calculate GLF sensitivity via the much simpler to calculate (local) buttressing number. Our analysis in section 4.3, which has been significantly revised and updated (including updated analysis and discussion of perturbations and the resulting changes that occur *at* the location of perturbations) is consistent with these conclusions. Throughout our revised section 4.3, we have attempted to clarify and emphasize the fundamental inconsistencies we find between the impacts of (1) local (at the grid cell) perturbations on various physical quantities, including the buttressing number, versus (2) changes in areas neighboring the immediate perturbation, versus (3) domain-integrated changes in buttressing and ice flux at the grounding line, and to more clearly tie the findings from this section of the paper to the broader discussion

and conclusions. In general, we show that, on the ice shelf, changes in buttressing at and immediately neighboring to perturbation locations are generally not consistent with our broader understanding for how buttressing works and also not consistent with the changes observed by the integrated ice shelf / ice sheet system explored here (i.e., local perturbations (reductions) in ice shelf thickness *reduce* overall ice shelf buttressing, which in turn *increases* overall ice flux across the grounding line).

Initially, I was willing to accept this judgment but then I realised that the same counter-intuitive response is seen in the principal strain-rate components (Fig.7e and f). These also indicate compression within the perturbed area (and slightly beyond). Consequently, you also need to dismiss the usefulness of this measure. This is too much of a stretch for me. I simply think that your analysis should consistently avoid areas close to the perturbations. To substantiate my view, I want to briefly explain the 1st principal buttressing or strain-rate changes in Fig7 e and g. After the perturbation, you clearly get less buttressing and increased extension upstream and downstream (in-flow direction) of the affected area. Sideways, but still along the 1st principal direction, these effects result in increased buttressing and compression (similar to a bottleneck effect). This explanation seems reasonable. I therefore strongly urge you to moderate and adjust your assessment of the buttressing metric, accordingly

This is a difficult argument to follow because, by nature, the buttressing number calculations are *local* in nature. It's hard to support their use on the basis of physical arguments if one cannot understand and connect local changes in buttressing to the broader changes in buttressing that control overall flux across the grounding line. Nevertheless, we go through a detailed analysis in our revised section 4.3 (and related Fig. 6) where we attempt to connect the local and neighboring impacts of perturbations on the shelf (including their impacts on buttressing number) to the broader changes in buttressing experienced by the entire ice shelf and their impacts on grounding line flux. While we can provide a fairly detailed narrative for *what* happens when a perturbation is applied to the ice shelf, we still lack a convincing physical understanding for *why* it happens. That is, why should the grounding link flux sensitivity -- an integrated quantity -- be correlated or adequately characterised by a locally calculated buttressing number on the ice shelf? We cannot confidently answer that question here, which gives us great hesitation in blindly applying these correlations. Moreover, our findings that many other easily derived physical quantities (some trivial, e.g. ice thickness) also correlate well with grounding line flux suggest that there may be no direct physical connection between these two quantities that would support their broader use (the correlations could be spurious or fortuitous, as discussed in newly added parts of Section 4.3.4 and discussion and Table S1 in the Supplementary Material). Regardless, we clearly show that these same correlations become weak and unconvincing when applied to realistic ice shelf domains. We would be happy for someone else to carry on with trying to further understand and justify the use of local buttressing numbers as part of ongoing work, but that is not the goal of our paper. The reviewer is suggesting that we come up with a better definition for, calculation of, and understanding of a buttressing number that takes non-local factors into account. This is a laudable goal, but again, is well outside the stated aims and scope of this paper.

A main motivation for why I raise this point is that many ice-flow models are not capable of an adjoint-based evaluation. It would therefore be constructive, if you could give some advice on how to best evaluate the local buttressing metric wrt. the GLF sensitivity. You nicely show that there is a correlation.

We fully appreciate this and, as stated above, it was a primary motivation when we initially undertook this study. Unfortunately, we cannot advocate further for the application of this method for the reasons argued above.

Your strategy to introduce a buffer zone around the grounding line is valuable (it is anyhow clear that these regions are important for the GLF sensitivity). From Fig.4, I think that areas with negative buttressing values should also be excluded (gives more flexibility than prescribed masking). So you could give some advise on how this metric can still be useful.

We have updated and improved the discussion of the necessary "buffer zone" in the revised manuscript. Specifically, we now introduce a more quantitative way of calculating this buffer zone based on the ratio of shear to normal stress (Section 4.1 and Fig. S2). Unfortunately, this does nothing to address the fundamental problems of needing a buffer zone in the first place; 1) this removes many of the most sensitive areas from consideration, and 2) when applied to realistic ice shelves, one is limited to a small area of the ice shelf if strong correlations are of interest.

Moreover, you should emphasise that if the interest is in the GLF sensitivity, the buttressing metric should be computed in p1/flow direction as against Furst et al. (2016). This comment further implies that you might want to reconsider the structure of the document: I suggest that you start with the GLF sensitivity of Reese et al. (2018). Then you could show that the adjoint-based approach gives equivalent results. Afterwards, you might want to assess the utility of the buttressing metrics (advice, limitations, etc.) to explain the GFL sensitivity

Indeed, we do clearly argue that buttressing calculated in the p1 and ice flow directions are better for quantifying the GLF sensitivity than the p2 direction, at least for the case where strong correlations are observed. We have not, however, opted to restructure our manuscript as suggested because our current conclusions and recommendations are better supported by the current organization and narrative.

<u>Minimum and maximum speed increase</u>

It took me a while to get my head around the retrieval of the direction of the minimal and maximal speed increase (L182ff). Although I am very impressed by the distinct peaks in the resultant distribution (Fig.6b), I wonder about its utility in this study. After its presentation, this measure is briefly compared to Gudmundson (2003) and shortly re-raised for the Larsen C

setup. It is not discussed nor mentioned in the conclusions. I therefore urge you to re-consider its utility

This section and the related figures have been removed from the revised version of the paper.

1. Please reduce the overall amount of footnotes. Sometimes they keep valuable extra information, which should appear in the text.

We have significantly reduced the number of footnotes by including most of the relevant material in the primary text.

2. Please introduce a figure of GLF response Nrp and the buttressing values (p1,p2, flow) for Larsen C. It might help you to delineate the area in which the GLF response and buttressing values are correlated.

This has been added as a third column of panels to a new figure that combines several figures from the original version of the manuscript. This information can now be found in Fig. S6 in the SI.

L29 The term 'longitudinal stresses' seem to be too narrow here. I would rather speak of 'membrane stresses' following Hindmarsh (2006).

Thanks for this suggestion. We have updated the manuscript accordingly.

L42 Delete 'of ice'

Done.

L60 Insert comma after parenthesis.

Corrected.

L115 This sentence is not true. You do not show the response on the southern/botton part of the MISMIP+ setup.

What is meant here is that we do analyze the response to perturbations over the entire model domain but we don't conduct perturbation experiments over the entire domain. This is because the response will be symmetric about the centerline. For example, the response of the change in GLF to a perturbation at (x,y)=(480 km, 50 km) will be the same as to a perturbation at (x,y)=(480 km,30 km), just mirrored about the ice stream / shelf centerline.

L118 As in the original study by Reese et al. (2018), I do not understand the meaning of P. You say it is the local mass change associated with the perturbation. So it should be rather constant

(despite element size variations on Larsen C). Units should be m 3 . The GL flux change R is however in units of m 3 /yr. I do not understand how Nrp can then be dimensionless. I think that I misunderstood the meaning of P. Please explain in more detail.

We have added more information to this section of the paper to clarify the units on both R and P. In Reese et al. (2018), it is implicit that the time period of interest is one year (according to personal communications). Therefore, P should have units of m^3, which are the same units as R. We have explicitly stated that the units of R and P are both in m^3 (in which case their ratio is non-dimensional).

L169 You must have noticed the dip in the correlation with the p1-buttressing (Fig. 5a). So the best correlation occurs at ±25◦ . With respect to the flow direction, the optimal correlation is ~100◦ turned (counterclockwise, Fig. 5b). Your statement in this line does note entirely hold.

We maintain that this statement is correct: if we move the curve in Fig. 5b to the right by around 50 degrees, the point with the best correlation in Fig. 5b moves to 150 deg, similar to the local maximum in Fig. 5a. The point with the second best correlation in Fig. 5b is shifted to ~210 deg, i.e., 30 deg, corresponding to the second local maximum in Fig 5a.

L173 You envoke the notion of an overall best buttressing metric. I do not think that this exists as such. It will depend on the spatial focus which can be the GL, central areas of the ice shelf or the calving front. Please remove this notion of a best metric.

The notion of a “best” metric is not ours but comes from the previous work of Fürst et al. (2016). We state this clearly in our paper. We’re not supporting its use or definition here. To avoid confusion, we have changed “best” to “good” in this sentence

L194-L207 Prior to this section, you focus on the speed-up signal ‘among neighbouring cells’ (L182-L194). In this section, you then discuss buttressing changes within the perturbed areas. This seems inconsistent. From Fig. 7g and h, I think you can extract a meaningful, aggregated index for buttressing changes excluding the perturbation centre. Upstream of the perturbation (in flow or p1 direction), the buttressing decreases with highest decrease close to the perturbed area. This inconsistent treatment therefore seems deliberate and strongly biases your interpretation. This bias leads to harsh judgments of the buttressing metric in the subsequent two sections, which are, in my opinion, note well justified. Please stay more objective. You also show the strain rates fields in the principal direction which also show overall compression within the perturbed zones. You do no discredit the usefulness of these values either.

We have updated the analysis and discussion in this entire section, including a focus on the impacts of perturbations exactly at the grid cells where perturbations are applied. As noted above, we agree that one can conduct a careful analysis of a single perturbation in order to understand how, overall, that perturbation leads to the broader changes in buttressing that are expressed as changes in GLF. However, we still lack a detailed understanding for how this

cause-and-effect is physically connected to the concept of a locally calculated buttressing number. We also show (in a new section in the SI) that similarly strong correlations exist between GLF and other physical quantities, some of which are unrelated to buttressing or buttressing number. This, and more importantly, the lack of strong correlations when exploring realistic ice shelf domains leads us to abandon further investigation of the utility of this method as a proxy for understanding GLF sensitivity.

L225-L238 This paragraph judges the results and it is therefore better located in the discussion conclusion. I also sense some redundancy.

This section (4.3.3), which has been significantly revised, is a necessary summary of our findings from the detailed analysis conducted in the sections immediately above it. Further, it is a necessary transition from discussion of the idealized MISMIP+ test case domain to the more realistic Larsen C domain.

L273-L289 This paragraph presents methodology so it should appear earlier (not as a sub-section of the Results).

While this change would make our paper more closely follow the strict formatting of a standard research paper (e.g., introduction, methods, results, conclusions) we think that the overall readability would suffer as a result. Further, a number of other reviewer comments indicate that the paper and interpretation would be easier to follow if this strict partitioning is avoided. Therefore, we opt to keep the formatting of these sections as they currently are.

Fig.1 Poor figure quality. Missing overview figure for localisation of Larsen C. What did you do about Bawden Ice Rise? Could you also show the observed velocity magnitude on Larsen C. Please indicate in the figure that the velocities you show, present the state after the relaxation (you only mention this in the text L105).

The location of Larsen C has been added to the figure. We have also added Figure S1 (to the Supplementary Material) showing the comparison between modeled and observed ice surface speeds on Larsen C. With respect to Bawden Ice Rise, we have looked into this in some detail and it appears that it is a small feature that does not show up in our domain due to our initial data interpolation onto a mesh with a minimum resolution of approximately the same size as this feature. We thank the reviewer for pointing this out, as it is something we will pay closer attention to including in future meshes.

Fig.2 In the caption you speak about 'perturbation points'. The perturbation does not affect a single point but an entire patch.

We now refer to these as "perturbed grid cells" instead of "perturbation points".

I would use different colours for the response number and buttressing metrics.

While we tried out multiple colorbars for the different panels in Fig. 2 (panel a vs. panels b, c, and d), we ultimately decided to keep them the same. This is primarily because it is then much easier to compare the spatial pattern of the GLF response number with the spatial patterns of the buttressing numbers in different directions (i.e., making a qualitative comparison by “eyeball”).

Why do you get negative response numbers for perturbations next to the grounding line?

We observe negative adjoint sensitivities only for cells intersecting the grounding line. For those cells, changes in thickness directly affect the grounding line position/length and the thickness over the GL, which could lead to negative responses. We have added a note to the Fig. 2 caption on the topic of negative response number. This topic is also discussed in the 4th paragraph of Section 4.5 (starting around line 331).

Figs.11&12 I would try to merge these figures. Panels (a) can be placed as an inset into panels (b).

As suggested, we have merged Figs. 11 and 12. They have also been moved into the SM (currently as Fig. S6).

Diagnosing the sensitivity of grounding line flux to changes in sub-ice shelf melting

Tong Zhang[1], Stephen F. Price[1], Matthew J. Hoffman[1], Mauro Perego[2], and Xylar Asay-Davis[1]

[1]Fluid Dynamics and Solid Mechanics Group, Los Alamos National Laboratory, Los Alamos, NM, 87545, USA
[2]Center for Computing Research, Sandia National Laboratories, Albuquerque, NM, 87185, USA

Correspondence: T. Zhang (tzhang@lanl.gov), S. Price (sprice@lanl.gov)

Abstract. ~~We seek to understand causal connections between changes in sub-ice shelf melting, ice shelf buttressing, and grounding-line flux.~~ Using a numerical ice flow model, we study changes in ice shelf buttressing and grounding line flux due to localized ice thickness perturbations~~—~~, a proxy for localized changes in sub-ice shelf melting~~—~~. From our experiments, applied to idealized (MISMIP+) and realistic (Larsen C) ~~domains. From our experiments~~ice shelf domains, we identify a correlation between a locally derived buttressing number on the ice shelf, based on the first principal stress, and changes in the integrated grounding line flux. The origin of this correlation, however, remains elusive from ~~a physical perspective; while local thickness perturbations on the ice shelf (thinning) generally correspond to local increases in buttressing, their integrated impact on changes at the grounding line are exactly the opposite (buttressing at the grounding line decreases and ice flux at the grounding line increases). This and additional complications encountered when examining realistic~~ the perspective of a theoretical or physically-based understanding. This and the fact the correlation is generally much poorer when applied to realistic ice shelf domains motivates us to seek an alternative approach~~,~~. We therefore propose an adjoint-based method for calculating the sensitivity of the integrated grounding line flux to local changes in ice shelf geometry. We show that the adjoint-based sensitivity is identical to that deduced from pointwise, diagnostic model perturbation experiments. Based on its much wider applicability and the significant computational savings, we propose that the adjoint-based method is ideally suited for assessing grounding line flux sensitivity to changes in sub-ice shelf melting.

1 Introduction

Marine ice sheets like that overlying West Antarctica (and to a lesser extent, portions of East Antarctica) are grounded below sea level and their bedrock would remain so even after full isostatic rebound (Bamber et al., 2009). This and the fact that ice sheets generally thicken inland leads to a geometric configuration prone to instability; a small increase in flux at the grounding line thins the ice there, leading to floatation, a retreat of the grounding line into deeper water, further increases in flux (due to still thicker ice), and further thinning and grounding line retreat. This theoretical "marine ice sheet instability" (MISI) mechanism (Mercer, 1978; Schoof, 2007) is supported by idealized ~~(e.g., Schoof, 2012; Asay-Davis et al., 2016)~~ (e.g., Schoof, 2007; Cornford et al., 202 realistic (e.g., Cornford et al., 2015; Royston and Gudmundsson, 2016) ice sheet modeling experiments, and some studies (Joughin et al., 2014; Rignot et al., 2014) argue that such an instability is currently under way for outlet glaciers of Antarctica's

Amundsen Sea Embayment~~(ASE)~~. The relevant perturbation for grounding line retreat in the ~~ASE~~ Amundsen Sea Embayment is thought to be intrusions of relatively warm, intermediate-depth ocean waters onto the continental shelves, which have reduced the thickness and extent of marginal ice shelves via increased sub-ice shelf melting (e.g., Jenkins et al., 2016). These reductions are important because fringing ice shelves restrain the flux of ice across their grounding lines farther upstream – the so-called "buttressing" effect of ice shelves (Gudmundsson et al., 2012; Gudmundsson, 2013; De Rydt et al., 2015) – which makes them a critical control on the rate of ice flux ~~from Antarctica to~~ across Antarctic grounding lines into the ocean.

On ice shelves, the driving stress (from ice thickness gradients) is balanced by gradients in ~~longitudinal stress~~ membrane stresses (Hutter, 1983; Morland, 1987; Schoof, 2007)~~and~~ . For an ice shelf in one horizontal dimension (x,z)~~provides~~ , these longitudinal stress gradients provide no buttressing (Schoof, 2007; Gudmundsson, 2013). For realistic, three-dimensional ice shelves, however, buttressing results from three main sources: 1) along-flow compression, 2) lateral shear, and 3) "hoop" stress (Wearing, 2016). Compressive and lateral shear stresses can provide resistance to extensional ice shelf flow through along- and across-flow stress gradients. The less commonly discussed "hoop" stress is a transverse stress arising from azimuthal extension in regions of diverging flow (Pegler and Worster, 2012; Wearing, 2016). Due to the complex geometries, kinematics, and dynamics of real ice shelves, an understanding of the specific processes and locations that control ice shelf buttressing is far from straightforward.

Several recent studies apply whole-Antarctic ice sheet models, optimized to present-day observations, towards improving our understanding of how Antarctic ice shelves impact ice dynamics farther upstream or limit flux across the grounding line. Fürst et al. (2016) proposed a locally derived "buttressing number" (extended from Gudmundsson, 2013) for Antarctic ice shelves and used it to guide the location of calving experiments whereby the removal of progressively larger portions of the shelves near the calving front identified dynamically "passive" ~~ice~~ shelf regions; removal of these regions (e.g., via calving) was found to have little impact on ice shelf dynamics or the flux of ice from ice upstream to the calving front. Reese et al. (2018) conducted a set of ~~forward model~~ diagnostic, forward-model, perturbation experiments to link small, localized decreases in ice shelf thickness to changes in integrated ~~grounding-line~~ grounding line flux (GLF), thereby providing a map of GLF sensitivity to local increases in sub-ice shelf melting.

Motivated by these studies, we build on and extend the methods and analysis of Fürst et al. (2016) and Reese et al. (2018) to address the following questions: (1) ~~Do local evaluations of ice shelf buttressing reflect how local perturbations in ice shelfthickness impact grounding line flux~~[1] ~~?~~ How do changes in ice-flux across the grounding line relate to local estimates of ice-shelf buttressing evaluated on the ice shelf? (2) What are the limitations of locally derived buttressing metrics when used to assess GLF sensitivity? (3) Can new methods overcome these limitations? Our specific goal is to identify robust methods for diagnosing where on an ice shelf changes in thickness (here, assumed to occur via increased sub-ice shelf melting) have a significant impact on flux across the grounding line. Our broader goal is to contribute to the understanding of how increased sub-ice shelf melting can be expected to impact the dynamics and stability of real ice sheets.

Below, we first provide a description of the ice sheet model used in our study and the model experiments performed. We then analyze and discuss the experimental results in order to quantify ~~how well~~ the correlation between easily evaluated, local

[1] ~~For example, are the local evaluations of buttressing from Fürst et al. (2016) related to the GLF changes modeled by Reese et al. (2018)?~~

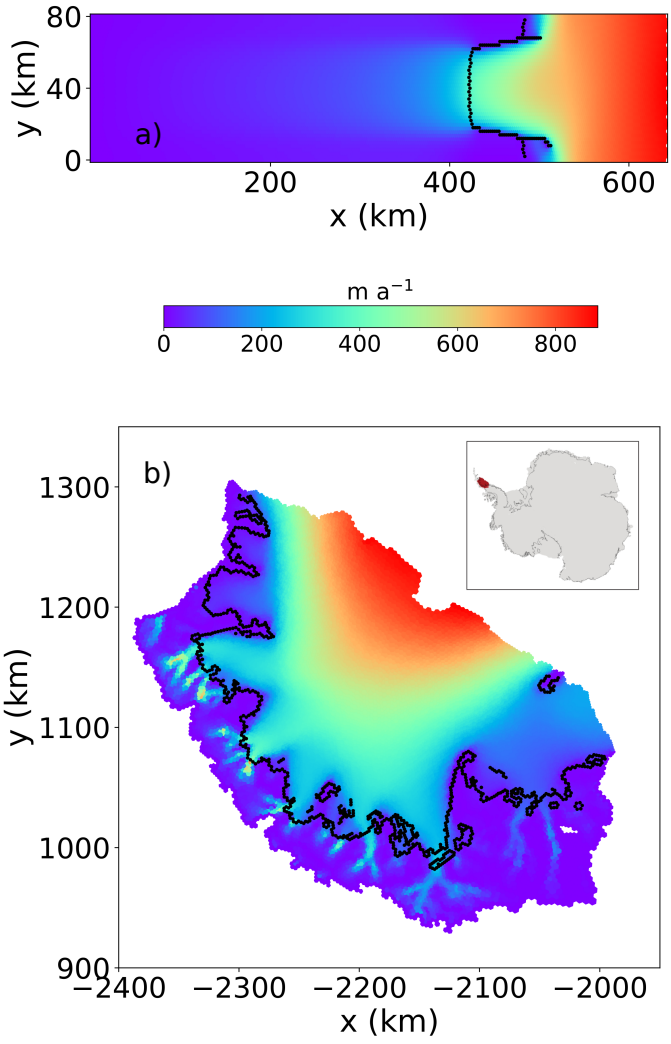

Figure 1. (a) Plan view of surface speed for the MISMIP+ and (b) Larsen C Ice Shelf experimental domains. For the Larsen C domain, velocities have been optimized to match observations from Rignot et al. (2011). Black curves indicate the location of the grounding line. The location of Larsen C Ice Shelf is shown as the shaded area in the inset in b). A comparison of modeled and observed ice surface speed is provided in Fig. S1.

buttressing metrics ~~correlate with~~ and modeled changes in GLF. This leads us to propose and explore an alternative, adjoint-
60 based method for assessing GLF sensitivity to ice shelf thickness perturbations. We conclude with a summary discussion and recommendations.

2 ~~Model description~~Numerical ice sheet model

2.1 Model description

We use the MPAS-Albany Land Ice model (MALI; Hoffman et al., 2018), which solves the three-dimensional, first-order approximation to the Stokes momentum balance for ice flow. Using the notation of Perego et al. (2012) and Tezaur et al. (2015a), this can be expressed as,

$$\begin{aligned} -\nabla\cdot(2\mu_e\dot{\boldsymbol{\epsilon}}_1)+\rho_i g\frac{\partial s}{\partial x} &= 0, \\ -\nabla\cdot(2\mu_e\dot{\boldsymbol{\epsilon}}_2)+\rho_i g\frac{\partial s}{\partial y} &= 0, \end{aligned} \tag{1}$$

where x and y are the horizontal coordinate vectors in a Cartesian reference frame, $s(x,y)$ is the ice surface elevation, ρ_i represents the ice density, g the acceleration due to gravity, and $\dot{\boldsymbol{\epsilon}}_{1,2}$ are given by

$$\dot{\boldsymbol{\epsilon}}_1 = \begin{pmatrix} 2\dot{\epsilon}_{xx}+\dot{\epsilon}_{yy}, & \dot{\epsilon}_{xy}, & \dot{\epsilon}_{xz} \end{pmatrix}^T, \tag{2}$$

and

$$\dot{\boldsymbol{\epsilon}}_2 = \begin{pmatrix} \dot{\epsilon}_{xy}, & \dot{\epsilon}_{xx}+2\dot{\epsilon}_{yy}, & \dot{\epsilon}_{yz} \end{pmatrix}^T. \tag{3}$$

The "effective" ice viscosity, μ_e in Eq. ~~(1)~~(1), is given by

$$\mu_e = \gamma A^{-\frac{1}{n}}\dot{\epsilon}_e^{\frac{1-n}{n}}, \tag{4}$$

where γ is an ice stiffness factor, A is a temperature-dependent rate factor, $n=3$ is the power-law exponent, and the effective strain rate, $\dot{\epsilon}_e$, is defined as

$$\dot{\epsilon}_e \equiv \left(\dot{\epsilon}_{xx}^2+\dot{\epsilon}_{yy}^2+\dot{\epsilon}_{xx}\dot{\epsilon}_{yy}+\dot{\epsilon}_{xy}^2+\dot{\epsilon}_{xz}^2+\dot{\epsilon}_{yz}^2\right)^{\frac{1}{2}}, \tag{5}$$

where $\dot{\epsilon}_{ij}$ are the corresponding strain-rate components.

Under the first-order approximation to the Stokes equations, a stress free upper surface can be enforced through

$$\dot{\boldsymbol{\epsilon}}_1\cdot\mathbf{n}=\dot{\boldsymbol{\epsilon}}_2\cdot\mathbf{n}=0, \tag{6}$$

where $\mathbf{n}$ is the outward pointing normal vector at the ice sheet upper surface, $z=s(x,y)$. The lower surface is allowed to slide according to the continuity of basal tractions,

$$2\mu_e\dot{\boldsymbol{\epsilon}}_1\cdot\mathbf{n}+\beta u=0, \quad 2\mu\dot{\boldsymbol{\epsilon}}_2\cdot\mathbf{n}+\beta v=0, \tag{7}$$

where β is a spatially variable friction coefficient, $2\mu_e\dot{\boldsymbol{\epsilon}}_{1,2}$ represent the viscous stresses, and $\boldsymbol{u}$ is the two-dimensional velocity vector (u, v). The field β is set to zero beneath floating ice and the basal traction is computed with the SEP3 method described in Seroussi et al. (2014). On lateral boundaries in contact with the ocean, the portion of the boundary above sea level is stress free while the portion below sea level feels the ocean hydrostatic pressure according to

$$2\mu_e\dot{\boldsymbol{\epsilon}}_1\cdot\mathbf{n}=\tfrac{1}{2}\rho_i g H\left(1-\tfrac{\rho_i}{\rho_w}\right)n_1, \quad 2\mu_e\dot{\boldsymbol{\epsilon}}_2\cdot\mathbf{n}=\tfrac{1}{2}\rho_i g H\left(1-\tfrac{\rho_i}{\rho_w}\right)n_2, \tag{8}$$

where $\mathbf{n}$ is the outward pointing normal vector to the lateral boundary (i.e., parallel to the (x, y) plane), ρ_w is the density of ocean water, and n_1 and n_2 are the x and y component of $\mathbf{n}$. A more complete description of the MALI model, including the implementations for mass and energy conservation, can be found in Hoffman et al. (2018). Additional details on the momentum balance solver can be found in Tezaur et al. (2015a, b).

~~Here, we~~

2.1.1 GLF computation

The grounding line (GL) is computed as the zero level-set of $\phi(x,y) := \rho_i H(x,y) + \rho_w b(x,y)$, where H and b are the continuous, piece-wise linear finite element fields for the thickness and the bed topography, respectively, defined on a triangulation of the domain at hand. As a consequence, the GL is a piece-wise linear curve, separating grounded ice (where $\phi(x,y) > 0$) from floating ice (where $\phi(x,y) < 0$). The flux F per unit width at a point on the GL is calculated as $F := H\bar{\boldsymbol{u}} \cdot \boldsymbol{n}_{GL}$, where $\bar{\boldsymbol{u}}$ is the vertically averaged velocity, and $\boldsymbol{n}_{GL}$ is the normal to the GL, pointing towards the floating ice region. The integrated grounding line flux, hereafter GLF, is the line integral of F along the GL and it has units [$\mathrm{m^3\ yr^{-1}}$]. We note that perturbations of the thickness far from the GL affect the GLF only through changes in the velocity field, whereas perturbations of the thickness at triangles intersecting the GL also directly affect ice thickness at the GL and, via the flotation condition, also possibly the position and length of the GL. We further note that ice rises in the model are also surrounded by grounding lines and require no special treatment.

2.2 Model configuration

We apply MALI to experiments on both idealized and realistic marine-ice sheet geometries. For our idealized domain and model state, we start from the equilibrium initial conditions for the MISMIP+ experiments with a mesh resolution of about 2 km, as described in Asay-Davis et al. (2016). For our realistic domain, we use Antarctica's Larsen C Ice Shelf and its upstream catchment area. For the Larsen C domain, the model state is based on the optimization of the ice stiffness (γ in Eq.~~(4)~~ (4)) and basal friction (β in Eq.~~(7)~~ (7)) coefficients in order to provide a best match between modeled and observed present-day velocities (Rignot et al., 2011) using adjoint-based methods discussed in Perego et al. (2014) and Hoffman et al. (2018). The domain geometry is based on Bedmap2 (Fretwell et al., 2013), and ice temperatures, which are used to determine the flow factor and held fixed for this study, are taken from Liefferinge and Pattyn (2013). Mesh resolution ~~on the ice shelf is between~~ is 2~~and 4 km~~ km at the grounding line and coarsens to 4 km near the calving front of the ice shelf and 5 km in the ice sheet interior. Following optimization to present-day velocities, the model is relaxed using a 100-year forward run, providing the initial condition from which the Larsen C experiments are conducted (as discussed below). The domain and initial conditions were extracted from the Antarctica-wide configuration used by MALI for initMIP experiments (Hoffman et al., 2018; Seroussi et al., 2019). Both the MISMIP+ and Larsen C experiments use 10 vertical layers that are finest near the bed and coarsen towards the surface. ~~The grounding line position is determined from hydrostatic equilibrium. A sub-element parameterization is used to define basal friction coefficient values at the grounding line (Seroussi et al., 2014).~~

3 Perturbation experiments

To explore the sensitivity of changes in GLF to small, localized changes in ice shelf thickness, we conduct ~~a number of~~ perturbation experiments analogous to those of Reese et al. (2018). Using diagnostic model solutions, we calculate the instantaneous ~~response of~~ change in GLF for the idealized geometry and initial state provided by the MISMIP+ experiment (Asay-Davis et al., 2016). We then conduct ~~a similar study~~ similar experiments for Antarctica's Larsen C Ice Shelf using a realistic configuration and initial state. The ~~geometry and steady-state~~ geometries and ice speeds for MISMIP+ (steady-state) and Larsen C Ice Shelf (present-day) are shown in Fig. 1.

Our experiments are conducted in a manner similar to those of Reese et al. (2018). We perturb the coupled ice sheet-shelf system by decreasing the ice thickness uniformly by 1~~m over~~ m at ice shelf grid cells (~~or square boxes containing a number of grid cells) covering the base of the ice shelves,~~ note that we consider the Voronoi grid dual to the Delaunay triangulation used by the finite element solver; every point of the Delaunay triangulation coresponds to a Voronoi cell), after which we examine the instantaneous impact on kinematics and dynamics (discussed further below). ~~For~~ For both the MISMIP+ ~~, we use a uniform hexagonal mesh with a horizontal resolution of around 2 km and we perturb the thickness at single cells in the mesh. For the Larsen C Ice Shelf, horizontal mesh resolution is spatially variable and – to maintain consistency with the experiments of Reese et al. (2018) – we assign each grid cell to fall within one and only one 20×20 km square perturbation "box", to which thickness perturbations are applied uniformly~~and Larsen C domains, the local ice shelf surface and basal elevations are adjusted following perturbations in order to maintain hydrostatic equilibrium. Lastly, for the MISMIP+ 2-km experiments, we note that, in order to save on computing costs, we only perturb the region of the ice shelf for which $x < 530$ km (the area over which the ice shelf is laterally buttressed) and for which $y > 40$ km (due to symmetry about the center line). We do, however, analyze the response to these perturbations over the entire model domain.

Similar to Reese et al. (2018), we define a GLF response number for our perturbation-based experiments,

$$N_{rp} = \frac{R}{P}, \tag{9}$$

where R is the change in the ~~ice (mass) flux integrated along the entire grounding line~~ GLF over a year due to a perturbation in the thickness at a single grid cell~~(or box of grid cells in the case of Larsen C)~~, and P is the local ~~mass~~ volume change associated with the perturbation. The subscript rp denotes the "response" from "perturbation" experiments[1]. Note that both R and P have units of m^3 so that N_{rp} is dimensionless.

~~Distal changes~~

Changes in GLF (quantified by N_{rp}) in response to a local change in ice shelf thickness are ~~assumed~~ expected to occur via changes in ice shelf buttressing, which generally acts to resist the flow of ice across the grounding line. To quantify the local ice shelf buttressing capacity, we calculate a dimensionless buttressing number, N_b, analogous to that from Gudmundsson (2013) and Fürst et al. (2016),

$$N_b(\mathbf{n}) = 1 - \frac{\mathrm{T_{nn}}}{N_0}, \tag{10}$$

[1] ~~To distinguish from other approaches to be discussed below.~~

where ~~$T_{nn} := \mathbf{n} \cdot \mathbf{T}\mathbf{n}$~~ $T_{nn} := \mathbf{n} \cdot \mathbf{T}\mathbf{n}$ is a scalar measure of the stress normal to the surface defined by $\mathbf{n}$. The two dimensional stress tensor $\mathbf{T}$ is computed according to the shallow shelf approximation and is defined in Eq. (A6). N_0 is the value ~~that~~ ~~T_{nn} would take~~ of T_{nn} if the ice was removed up to the considered location and replaced with ocean water [1], ~~and it is defined as $N_0 := \frac{1}{2}\rho_i(1-\rho_i/\rho_w)gH$,~~ (or alternatively, the resistance provided by a static, neighboring column of floating ice at hydrostatic equilibrium) defined by

$$N_0 := \frac{1}{2}\rho_i g\left(1-\frac{\rho_i}{\rho_w}\right)H, \tag{11}$$

with ρ_i and ρ_w being the densities of ice and ocean water, respectively[1]. For the MISMIP+ experiment, ρ_i=918 kg m^{-3} and for the Larsen C experiment, ρ_i=910 kg m^{-3}. For both experiments, ρ_w=1028 kg m^{-3}. We elaborate further on the calculation of the buttressing number in Appendix A. While Gudmundsson (2013) chose the unit vector $\mathbf{n}$ to be normal to the grounding line to define the "normal" buttressing number, Fürst et al. (2016) extended his definition to the ice shelf by examining $N_b(\mathbf{n})$ for $\mathbf{n}$ along the ice flow direction and along the direction of the second principal stress. Here, we explore the connection between changes in grounding line flux (quantified by N_{rp}), sub-shelf melting, and local buttressing on the ice shelf (quantified by N_b[1]) corresponding to arbitrary $\mathbf{n}$ (in order to consider all possible relationships on the ice shelf). ~~Below, we refer to T_{nn} as~~ Note that we do not discuss the tangential buttressing number defined by Gudmundsson (2013); hereafter, we use "buttressing number" to refer exclusively to the "normal ~~stress". The tensor $\mathbf{T}$ is defined as follows, based on the two dimensional shallow shelf approximation~~[1], ~~

$$\mathbf{T} = \begin{Bmatrix} 4\mu_e\dot{\epsilon}_{xx} + 2\mu_e\dot{\epsilon}_{yy} & 2\mu_e\dot{\epsilon}_{xy} \\ 2\mu_e\dot{\epsilon}_{yx} & 4\mu_e\dot{\epsilon}_{yy} + 2\mu_e\dot{\epsilon}_{xx} \end{Bmatrix}.$$

~~

buttressing number", as defined above. ~~We elaborate further on the calculation of the buttressing numberin Appendix A. Additional details of ice shelf dynamics based on the shallow shelf approximation can be found in Greve and Blatter (2009).~~

4 Results

4.1 Correlation between buttressing and changes in GLF

A decrease in ice shelf buttressing tends to lead to an increase in GLF (e.g., Gagliardini et al., 2010, also see Fig. 2a) and intuitively we expect that the GLF should be relatively more sensitive to ice shelf thinning in regions of relatively larger buttressing. We aim to better understand and quantify the relationship between the local ice shelf buttressing "strength" in

[1] ~~Or alternatively, the resistance provided by a static, neighboring column of floating ice at hydrostatic equilibrium.~~

[1] ~~For the MISMIP+ experiment, ρ_i=918 kg m^{-3} and for the Larsen C experiment, ρ_i=910 kg m^{-3}. For both experiments, ρ_w=1028 kg m^{-3}.~~

[1] ~~Note that we do not discuss the tangential buttressing number defined by Gudmundsson (2013)). Hereafter, we use "buttressing number" to refer exclusively to the "normal buttressing number", as defined above.~~

[1] ~~While we employ a three-dimensional, first-order Stokes approximation here (Tezaur et al., 2015a), the depth-varying and depth-averaged solutions converge to the same value on ice shelves, where basal resistance is zero.~~

a given direction (characterized by N_b) and changes in GLF (characterized by N_{rp}). A reasonable hypothesis is that, for a given ice thickness perturbation, the resulting change in the GLF is proportional to the buttressing number at the perturbation location.

In Fig. 2, we show the results from all (730) perturbation experiments for MISMIP+, and the corresponding N_{rp} and N_b values. ~~For~~ We show values of N_b ~~, we show the values corresponding to~~ for three different directions, corresponding to the choice of $\mathbf{n}$ in Eq. ~~(10);~~ (10): the first principal stress direction ($\mathbf{n}_{p1}$), the second principal stress direction ($\mathbf{n}_{p2}$), and the ice flow direction ($\mathbf{n}_f$). In the discussion below, we frequently refer to these three directions when discussing the buttressing number. In agreement with the findings of Fürst et al. (2016), the largest values for N_b occur when it is calculated in the $\mathbf{n}_{p2}$ direction. While there appears to be a qualitatively reasonable spatial correlation between the magnitude of N_{rp} and N_b when the latter is calculated in the ~~$\mathbf{n}_{p1}$ and~~ $\mathbf{n}_{p2}$ and $\mathbf{n}_f$ directions (and less so when calculated in the ~~$\mathbf{n}_f$~~ $\mathbf{n}_{p1}$ direction), in Fig. 3 we show that there is no clear relationship between the response number N_{rp} and the buttressing number N_b calculated along any of these directions, at least for the case where we consider all points on the ice shelf.

In Fig. 4, ~~however,~~ we show correlations ~~(Figs. 4b–d)~~ between the modeled value of N_{rp} and N_b where we ~~have removed points for which the flow is weakly buttressed~~ ignore points meeting the following critera: (i) points where the ice shelf becomes unconfined ($x > 480$ km~~, where the ice shelf starts to become unconfined)~~); (ii) points within 2 cells from the GL; (iii) points where shear stresses are large according to the metric,

$$m_s = \frac{|\sigma_{p1} - \sigma_{p2}|}{|\sigma_{p1} + \sigma_{p2}|} \tag{12}$$

where σ_{p1} and ~~where the minimum distance to~~ σ_{p2} are the first and second principal normal stresses, respectively, and m_s is the ratio of the maximum shear stress to the mean normal stress. For the case of (i), a good correlation between N_b and N_{rp} is not expected for unconfined flow where buttressing is insignificant (Van Der Veen, 2013). For the case of (ii), complications near the grounding line ~~is less then 12 km (Fig. 4a). In this case, stronger, near-linear $N_{rp} : N_b$ relationships~~ (e.g., grounding line movement and geometry change associated with thickness perturbations, as noted in 2.1.1) may give incorrect GLF response numbers. For the case of (iii), we expect a relatively poor correlation between N_b and N_{rp} for locations where buttressing occurs primarily via lateral drag, which will be poorly captured by a stress metric (i.e., buttressing number) associated with a single direction. In a principal stress framework, shear stress is described by perpendicular normal stresses of opposite sign. Applying this metric means that we only evaluate correlations between N_b and N_{rp} for points where m_s from Eq. (**??**) is < 1 (i.e., where normal stress is dominant over shear stress; see also Fig. S2). When applying criteria (i)-(iii) above as a spatial filter, the number of points considered is reduced (Fig. 4a) and stronger correlations between N_{rp} and N_b emerge. In particular, a stronger correlation between N_{rp} and N_b occurs when N_b is calculated using $\mathbf{n}_{p1}$ (Fig. 4b) or $\mathbf{n}_f$ (Fig. 4d), relative to when using $\mathbf{n}_{p2}$ (Fig. 4c)~~or $\mathbf{n}_f$ (Fig. 4d)~~.

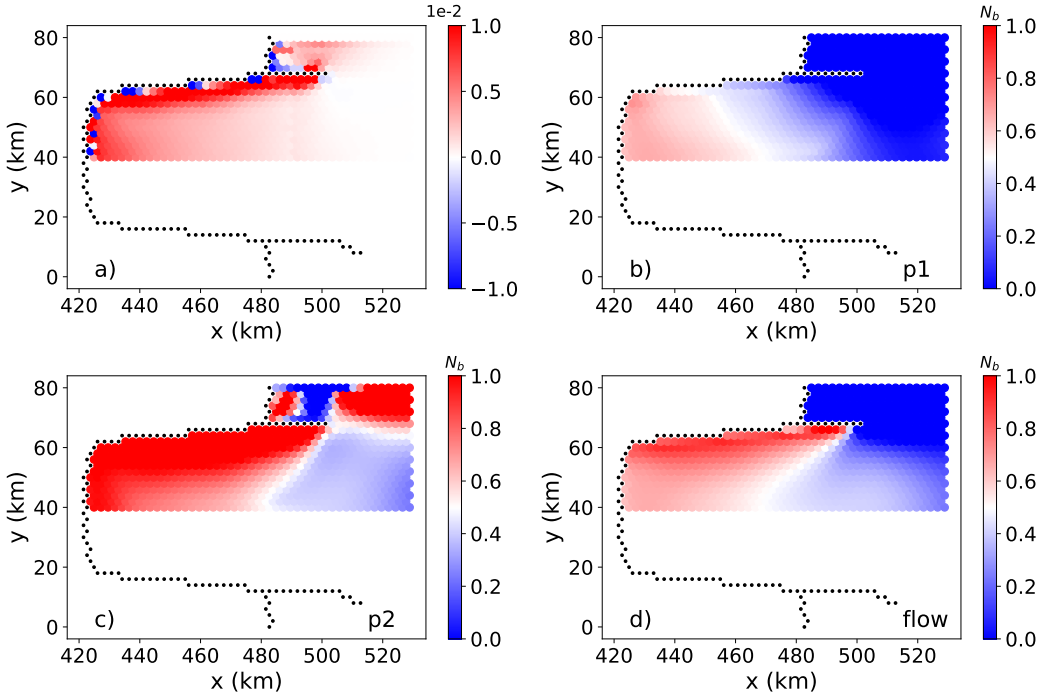

Figure 2. ~~The 730 perturbation points~~ GLF number and buttressing number for each of the 730 perturbed grid cells in the MISMIP+ experiments. (a) The spatial distribution of the GLF response number, N_{rp}. (b-d) The spatial distribution of the buttressing number, N_b, corresponding to directions (b) $\mathbf{n}_{p1}$, (c) $\mathbf{n}_{p2}$, and (d) $\mathbf{n}_f$. Black dots indicate grid cells located along the grounding line. The negative N_{rp} values in (a) correspond to a few partially-grounded cells in the vicinity of the GL, where the GLF can be reduced by ice shelf thinning. Here the colorbars for (a)–(d) do not show the full data range. Note that the negative GLF numbers in panel (a) are due to the nonlinear impacts of changes in both ice thickness and velocity at the GL.

4.2 Directional dependence of buttressing

The buttressing number at any perturbation point depends on ~~T_{nn}~~$\mathrm{T}_{\mathbf{nn}}$, which in turn depends on the chosen direction of the normal vector, $\mathbf{n}$ (Eq.~~10~~ (10)). Fürst et al. (2016) calculated N_b using $\mathbf{n}_f$ and $\mathbf{n}_{p2}$ and chose the latter – the direction corresponding to the second principal stress (the maximum compressive stress or the least extensional stress) – to quantify the local value of "maximum buttressing" on an ice shelf. In Fig. 5a, we plot the linear-regression correlation coefficients (r) for the $N_{rp} : N_b$ relationship where the direction of $\mathbf{n}$ used in the calculation of ~~T_{nn}~~$\mathrm{T}_{\mathbf{nn}}$ varies continuously from $\Delta\phi$ =0–180° relative to $\mathbf{n}_{p1}$ (we also show how the buttressing number N_b varies ~~according to direction , starting from $\mathbf{n}_{p1}$,~~ as a function of direction in Fig. S3). We find large correlation coefficients ($r > 0.9$) when N_b is aligned closely with $\mathbf{n}_{p1}$ ($\Delta\phi = 0°$ or 180°) and the smallest correlation coefficient ($r < 0.5$) when N_b is aligned with $\mathbf{n}_{p2}$ ($\Delta\phi = 90°$). Similar conclusions can be reached when examining the ~~continuous values for~~ variation of r with respect to the ice flow direction (Fig. 5b), where correlations are phase shifted by approximately 50° counter-clockwise relative to Fig. 5a. Clearly, the best correlation occurs along ~~the~~

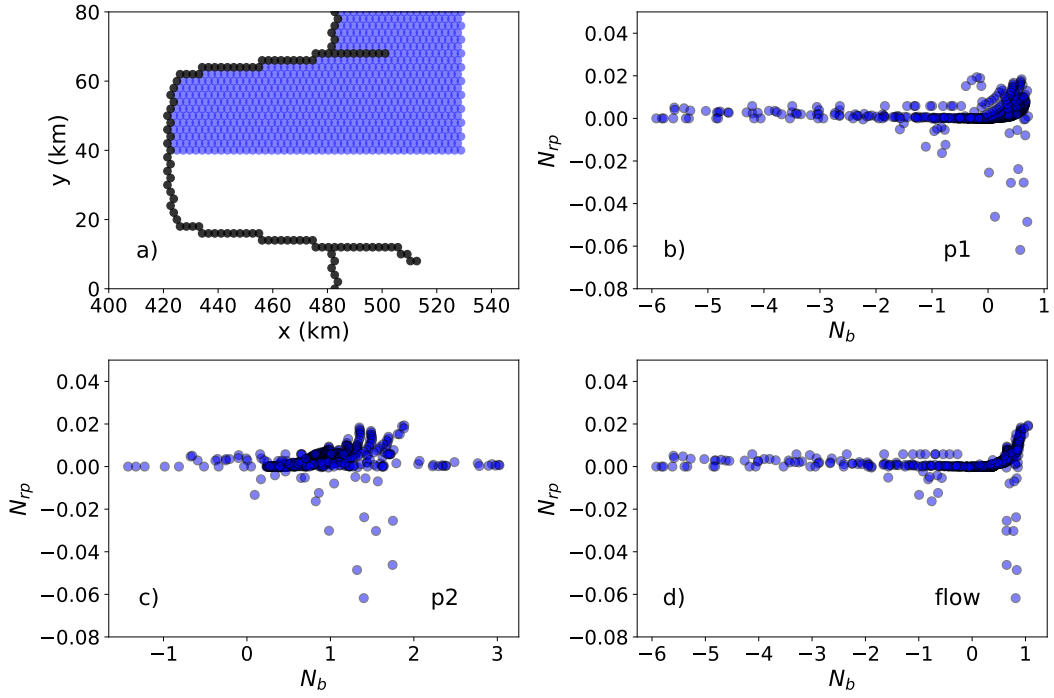

Figure 3. (a) Blue dots represent the locations of all perturbation points analyzed (730) for the $N_{rp} : N_b$ linear regression analysis. Black dots indicate grid cells located along the grounding line. (b-d) Modeled N_{rp} from perturbation experiments versus predicted N_{rp} as a function of N_b calculated along (b) $\mathbf{n}_{p1}$, (c) $\mathbf{n}_{p2}$, and (d) $\mathbf{n}_f$.

~~direction~~ a direction somewhere between $\mathbf{n}_{p1}$ and $\mathbf{n}_f$. Note that we do not see an exact match between Fig. 5a and Fig. 5b if we shift the angle by 50° because the angular difference between $\mathbf{n}_{p1}$ and $\mathbf{n}_f$ varies ~~slightly between individual grid cells where thickness perturbations are applied (distributions for the angular difference between n_{p1} and n_f are shown in Fig. ??).~~ for the perturbation locations analyzed.

Fürst et al. (2016) posit that $N_b(\mathbf{n}_{p2})$ provides ~~the best~~ a good local buttressing metric and chose it for identifying regions of maximum buttressing on an ice shelf ~~. Here, however~~with the goal of identifying "passive" ice that can be removed without tangibly affecting the remaining ice. While our results also show that buttressing is greatest in the direction of the second principal stress (which follows from the definitions of the second principal stress and the buttressing number, see also Fig. S3), we find that ~~,~~ buttressing in this direction is not useful for predicting changes in GLF; compared to $N_b(\mathbf{n}_{p2})$, $N_b(\mathbf{n}_{p1})$ and $N_b(\mathbf{n}_f)$ both show a better correlation with changes in GLF via local, sub-ice shelf melt perturbations. We ~~return to and~~ discuss these differences further ~~below~~ in Section 5.

4.3 ~~Local~~Perturbation impacts: local, far-field, and integrated ~~impacts of~~ changes~~in buttressing~~

~~We now examine how local~~

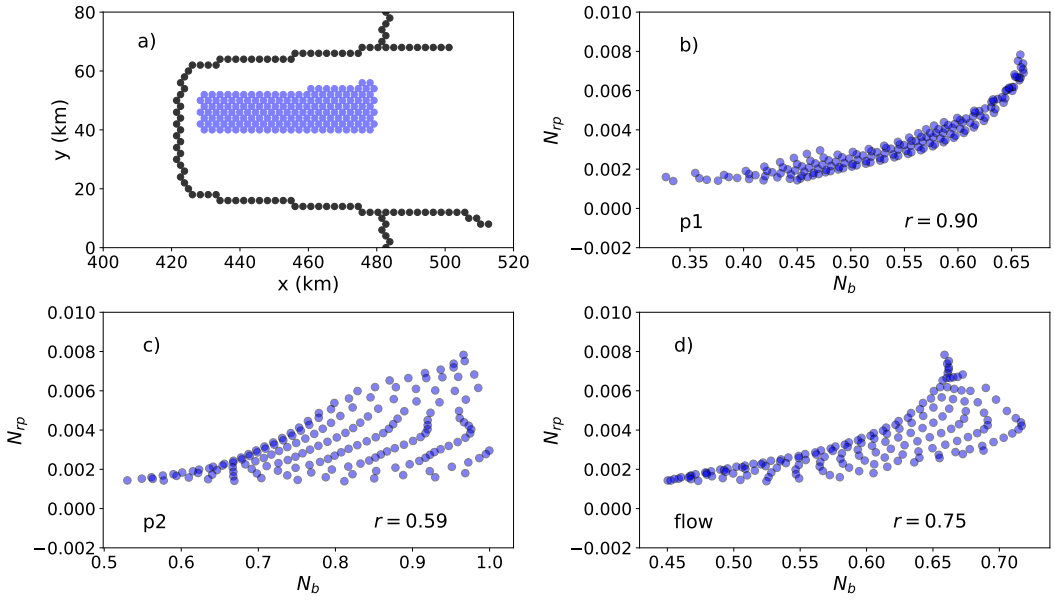

Figure 4. (a) Blue dots represent the locations of all perturbation points analyzed (~~142~~168) for the $N_{rp} : N_b$ linear regression analysis, based on the filtering criteria discussed in Section 4.1. Black dots indicate grid cells located along the grounding line. (b-d) Modeled N_{rp} from perturbation experiments versus predicted N_{rp} as a function of N_b calculated along (b) $\mathbf{n}_{p1}$, (c) $\mathbf{n}_{p2}$, and (d) $\mathbf{n}_f$. The correlation coefficient for each modeled N_{rp} versus N_b is given by r.

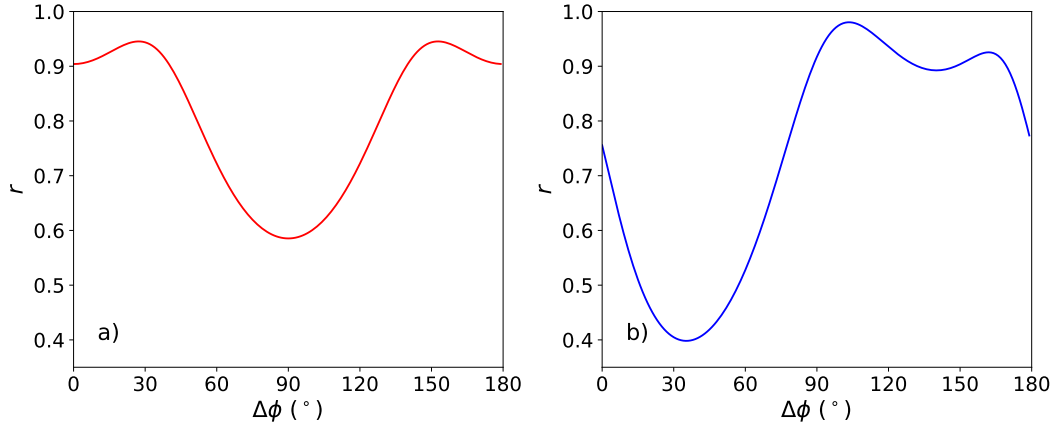

Figure 5. Correlation coefficients for the linear regression relationship of $N_{rp} : N_b$ where $\mathbf{n}$ is rotated counterclockwise by $\Delta\phi$ degrees relative to (a) $\mathbf{n}_{p1}$ and (b) $\mathbf{n}_f$. The perturbation points analyzed here are the same as in Fig. 4a.

We now look more carefully at thickness perturbations on the ice shelf ~~lead to local changes in geometry and velocity, and in turn, localchanges in buttressing. Our aim is to better understand how perturbations affect buttressing locally (on the ice shelf) and, in turn, impact the overall buttressing and ice flux at the grounding line.~~

4.3.1 ~~Changes in geometry, velocity, and buttressing in the vicinity of ice shelf thickness perturbations~~

~~To better understand the local impacts of a perturbation on the local ice velocity at each perturbation location, we calculate both the maximum and the minimum increase in ice speed[1] among neighboring cells (i.e., two values for each perturbation point) and the orientation of these neighboring cells relative to the $\mathbf{n}_{p1}$ and $\mathbf{n}_f$ direction at the perturbation point. The results are plotted as histograms in Fig. ??. Note that for our hexagonal mesh, there are six neighboring cells adjacent to each perturbed cell so that only a discrete number of directions (6) can be examined. The maximum and minimum speed increases cluster at 0–45° and near 60–90° relative to $\mathbf{n}_{p1}$, respectively (Fig. ??a). A similar relationship is seen in Fig. ??b, where the maximum and minimum speed increases cluster near 0°~~ in terms of their local, far-field, and ~~60°, respectively, relative to $\mathbf{n}_f$. Hence, the maximum ice speed increases near a perturbation are generally more closely aligned with the $\mathbf{n}_{p1}$~~ integrated impacts on changes in geometry, velocity, stress, buttressing, and ~~$\mathbf{n}_f$ directions and minimum ice speed increases are more closely aligned with the $\mathbf{n}_{p2}$ direction[1]. This suggests that local ice shelf thickness perturbations induce local speed changes along a favored direction, which here aligns closely with the ice flow direction, or $\mathbf{n}_f$. This finding is supported by Gudmundsson (2003), who used an idealized ice flow model experiment to demonstrate that, following perturbations to the basal roughness or slipperiness, the group velocity of that perturbation propagates primarily along the main ice flow direction.~~

~~Histograms for the maximum (red) and minimum (blue) percent speed increases in grid cells adjacent to a thickness perturbation point, plotted as a function of angular distance with respect to (a) $\mathbf{n}_{p1}$ and (b) $\mathbf{n}_f$. Points analyzed are those from Fig. 4a.~~

GLF.

4.3.1 Local perturbation impacts

Local thickness perturbations on the ice shelf alter the local ice thickness gradient; on the upstream ~~(grounding line)~~ side of the perturbation, ~~the thickness gradient will decrease and~~ it becomes more negative while on the downstream ~~(calving front) side it will increase~~ side it becomes less negative (Fig. 6a, b). ~~Locally, the result is an increase in~~ These thickness gradient changes increase the ice speed immediately upstream from the perturbation and decrease it immediately downstream of the perturbation (Fig. 6c), resulting in anomalous flow convergence towards the perturbation location (Fig. 6d). The resulting impacts on the principal strain rates (and thus the principal stresses) are increased compression (or ~~a decrease in~~ decreased extension) along

[1] ~~Here, we use speed changes as a proxy for changes in the local ice flux near perturbation points on the ice shelf because, (1) thickness changes are minimal and (2) changes in speed can be approximately interpreted as changes in velocity because directional changes are small.~~

[1] ~~Note that neighboring cells to a perturbation are distributed along discrete angles, so that there are generally not neighboring cells exactly along the $\mathbf{n}_{p2}$ direction.~~

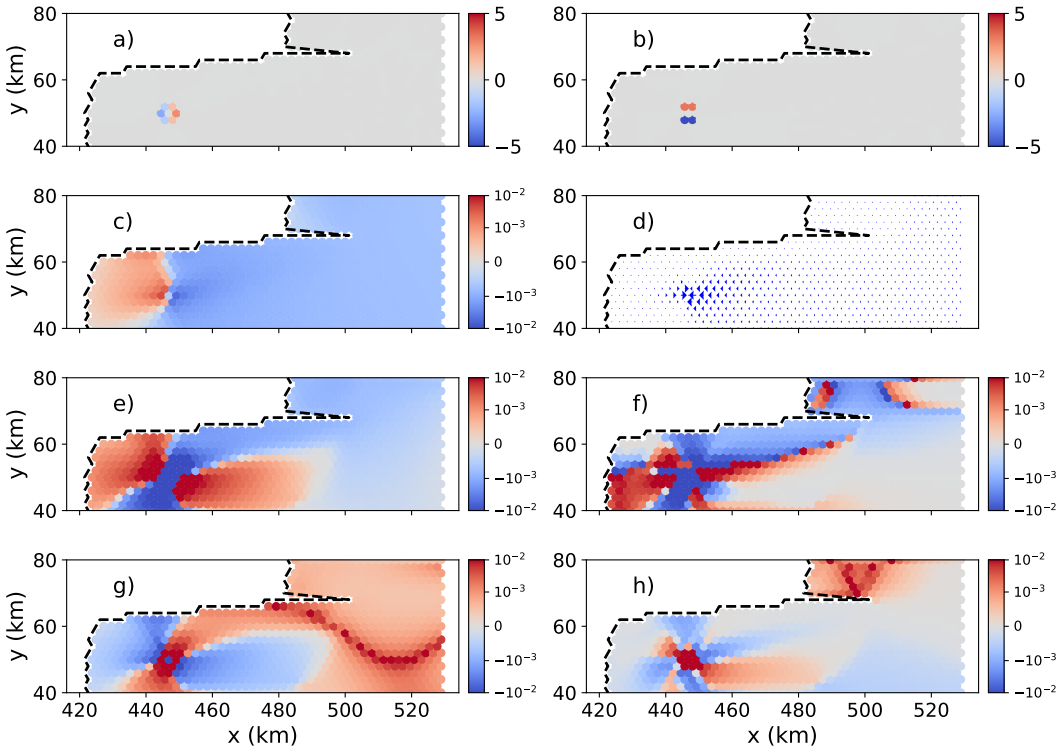

Figure 6. An example of the local change (ratio, in %) in (a) the ice thickness gradient in x, (b) ice thickness gradient in y, (c) ice speed, (d) ice velocity (relative), (e, f) principal strain rates, and (g, h) buttressing number following a local perturbation to the ice shelf thickness. In (e) and (g), changes (colors) are associated with the $\mathbf{n}_{p1}$ direction and for (f) and (h) changes are associated with the $\mathbf{n}_{p2}$ direction. ~~The white- and black-dashed lines show the direction of $\mathbf{n}_{p1}$ and $\mathbf{n}_{p2}$ at the perturbation location, respectively.~~

both principal ~~stress~~ directions (Fig. 6e, f) and, via Eq. ~~(10)~~(10), a corresponding increase in the local ~~buttressing number calculated~~ value of N_b along both principal stress directions (Fig. 6g, h).

~~Importantly, while we find that the overall spatial pattern of the change in buttressing is quite complex, variable, and depends on the location of the perturbation, the general pattern of the local change (at or within a few grid cells of the applied perturbation) is that of an *increase* in the buttressing number (see also~~ These spatial patterns of change are robust for a number of different perturbation points on the ice shelf (see Figs. S4 and S5 in the Supplementary ~~, analagous to Fig. 6, which show similar patterns but for different perturbation locations). This is further confirmed in~~ Material).

An important caveat applies to the grid cell associated with the location of the perturbation itself, where a decrease in N_b is seen, sometimes for only the $\mathbf{n}_{p1}$ direction but other times for both principal directions (Fig. S5). In Fig. 7, ~~where we show that, in response to local ice shelf thickness perturbations, for all~~ we quantify the local (at the perturbation location; Fig. 7a) and neighboring (immediately surrounding the perturbation location; Fig. 7b) changes in N_b for all of the points analyzed in Fig. 4 ~~there is an~~ and for all possible directions. From Fig. 7, we make two conclusions: 1) the local change in N_b is generally more

~~The change in buttressing number ΔN_b at the neighboring cells with maximum ice speed increase at all perturbation points. Changes in buttressing are calculated along the direction $\Delta\phi$, rotated counterclockwise relative to the $\mathbf{n}_{p1}$ direction. The points analyzed include those in Fig. 4a, which are shown as the shaded area, with the solid curve representing their mean value.~~

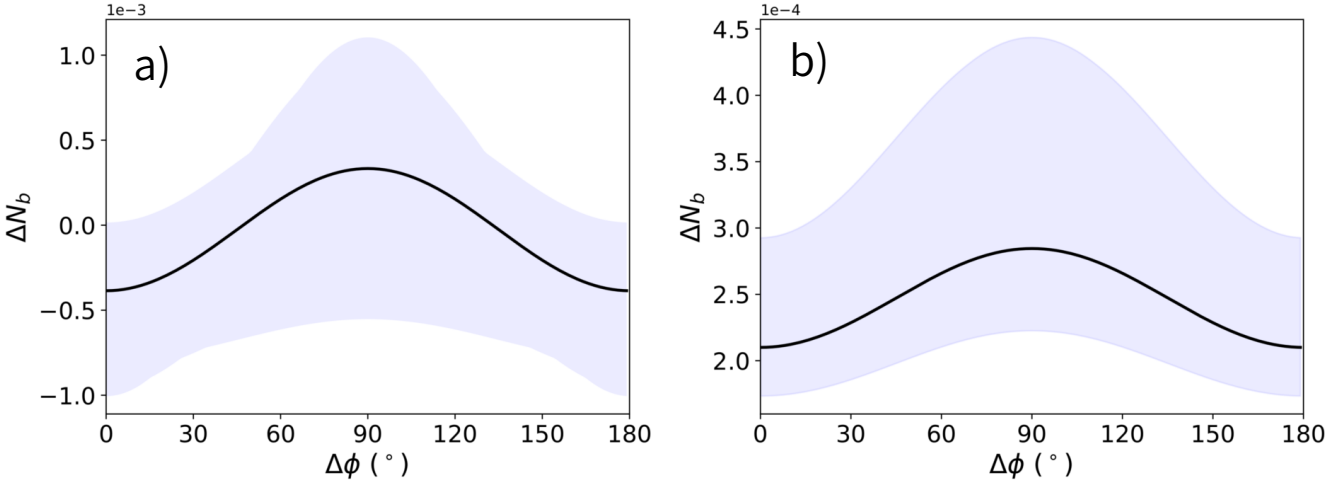

Figure 7. The change in buttressing number, ΔN_b, at and near to ice shelf thickness perturbations. In (a), the change at the perturbation location is shown and in (b) the mean change in all immediately neighboring cells is shown. Changes in buttressing are calculated along the direction $\Delta\phi$, rotated counterclockwise relative to the $\mathbf{n}_{p1}$ direction. The points analyzed include those in Fig. 4a, which are shown as the shaded area, with the solid curve representing their mean value.

positive along the $\mathbf{n}_{p2}$ direction (indicating a local *increase* in buttressing accompanying a thickness perturbation) and 2) the local and neighboring changes in buttressing are often inconsistent (i.e., a *decrease* in N_b at a particular grid cell coincides with an *increase* in ~~the buttressing number associated with both the $\mathbf{n}_{p1}$ and $\mathbf{n}_{p2}$ directions, and for every direction in between (the larger increase in~~ N_b in the neighboring cells). The first conclusion would seem to argue against using $N_b(\mathbf{n}_{p2})$ for quantifying local changes in buttressing in terms of their broader impacts on GLF (because, surprisingly, local thinning perturbations are more likely to indicate a local *increase* in buttressing along the $\mathbf{n}_{p2}$ direction~~emphasizes that the local ice flow is always more compressive (or less extensional)along the $\mathbf{n}_{p2}$ direction).As we discuss next, this finding of locally increased buttressing for all perturbations applied to the ice shelf is at odds with our desire to interpret the local buttressing number in terms of changes in GLF.~~

). The second conclusion suggests that analysis over wider spatial scales may be necessary for a consistent understanding of how local ice shelf perturbations impact GLF.

4.3.2 Far-field perturbation impacts

Away from the immediate vicinity of ice shelf thickness perturbations (i.e., beyond the grid cell where perturbations are applied and its immediate neighbors), the resulting changes are more uniform and easier to interpret. The broader pattern of

increased ice speed upstream from a perturbation location can be seen to extend spatially and diffuse with increased distance (Fig. 6c). Similar can be observed with respect to changes in principal strain rates and buttressing, at least for the $\mathbf{n}_{p1}$ direction (Figs. 6e and g), where a wide swath of increased extension and decreased local buttressing (as quantified by reductions in $N_b(\mathbf{n}_{p1})$) coincides with the region of increased ice speed extending upstream to the grounding line. This implied causality – a reduction in buttressing on the shelf leads to an increase in GLF upstream – is consistent with our understanding of ice shelf buttressing. Importantly, we note that a similar understanding based on changes in the $\mathbf{n}_{p2}$ direction (Figs. 6f and h) is much less straightforward due to more complicated spatial patterns and no obvious consistency between reductions in $N_b(\mathbf{n}_{p2})$ and the increases in ice speed that would lead to a corresponding increase in GLF. This interpretation of the far-field effects of local ice shelf perturbations is consistent when perturbations are applied at a number of different locations on the ice shelf (see Figs. S4 and S5 in the Supplementary Material).

A reasonable hypothesis is that the apparent correlation between $N_b(\mathbf{n}_{p1})$ and N_{rp} in Fig. 4b arises because of the connection, discussed above, between local thickness perturbations, far-field changes in principal stresses and buttressing along the $\mathbf{n}_{p1}$ direction, and increases in ice speed upstream of the perturbation. Similarly, the lack of such a clear connection for local perturbations and principal stresses and buttressing along the $\mathbf{n}_{p2}$ direction may account for the relatively poorer correlation between $N_b(\mathbf{n}_{p2})$ and N_{rp} shown in Fig. 4c. Next, we explore how these far-field changes are expressed at the grounding line.

4.3.3 ~~Changes in~~ Perturbation impacts on buttressing and ice flux at the grounding line

To understand how ~~perturbations propagate across the ice shelf and impact the grounding line, we~~ local perturbations in ice shelf thickness impact GLF, we now examine changes in the buttressing number and ~~the ice speed~~ ice speed at and normal to the grounding line~~following local perturbations in thickness on the ice shelf~~. To quantify this relationship, we define Υ_{gl},

$$\Upsilon_{\mathrm{gl}} = \mathrm{Corr}\left(\Delta\mathbf{N_b}, \Delta\mathbf{u}\right) = \frac{\mathrm{cov}\left(\Delta\mathbf{N_b}, \Delta\mathbf{u}\right)}{\sigma(\Delta\mathbf{N_b})\sigma(\Delta\mathbf{u})} \frac{\mathrm{cov}\left(\Delta\mathbf{N_b}, \Delta\mathbf{u}\right)}{s(\Delta\mathbf{N_b})s(\Delta\mathbf{u})}, \tag{13}$$

where $\Delta\mathbf{N_b} = \mathbf{N_{bp}} - \mathbf{N_{bc}}$ and $\Delta\mathbf{u} = \mathbf{u_p} - \mathbf{u_c}$ and with the subscripts p and c denoting the ~~perturbation and the~~ "perturbed" and "control" (i.e., ~~the initialcondition) experiments~~initial) model states, respectively. $\Delta\mathbf{N_b}$ and $\Delta\mathbf{u}$ denote vectors of the ~~changes~~ *changes* in the buttressing number and ~~the ice speed~~ ice speed normal to the GL, respectively, for all GL cells along the ~~grounding line~~main trunk of the ice stream (red points in Fig. 8). Υ_{gl}, a correlation coefficient, is an integrated [1] measure of the consistency between the magnitude and the sign of the change in ~~the~~ buttressing number and ice speed between the control and perturbation experiments, with cov and ~~σ~~ s representing the covariance and the standard deviation, respectively.

By plotting values of Υ_{gl} mapped to their respective perturbation locations on the ice shelf (Fig. 8), we show ~~that~~ there is generally a *negative* correlation between speed and buttressing at the GL: ~~*increases* in~~ in response to a thickness perturbation on the ice shelf, buttressing *decreases* and speed (and hence flux) across the GL ~~correlate with *decreasesin buttressing at the GL (increases*~~, in line with our general understanding of buttressing. In Fig. 8~~).This negative correlation is substantially stronger when the buttressing number is~~ a, we show a reference case for which T_{nn} in Eq. (10) (and hence in Eq. (13)) is calculated

[1] ~~Integrated in the sense that the correlation coefficient takes into account the entire grounding line.~~

normal to the grounding line. In this case, the N_b values in Eq. (13) are calculated along the ~~$\mathbf{n}_{p1}$ direction~~ GL as defined by Gudmundsson (2013) ($\Upsilon_{\rm gl} = \Upsilon_{\rm gl}(\mathbf{n}_{gl})$, where $\mathbf{n}_{gl}$ is the direction normal to the grounding line). In Fig. 8b and c, we show $\Upsilon_{\rm gl}(\mathbf{n}_{p1})$ and $\Upsilon_{\rm gl}(\mathbf{n}_{p2})$, respectively. As expected, the correlation is strongly negative for $\Upsilon_{\rm gl}(\mathbf{n}_{gl})$ (Fig. 8a) ~~than along the $\mathbf{n}_{p2}$ direction~~and we find that $\Upsilon_{\rm gl}(\mathbf{n}_{p1})$ is a close match (Fig. 8b). While much of the shelf under consideration also shows a negative correlation for $\Upsilon_{\rm gl}(\mathbf{n}_{p2})$, the correlations are generally weaker and there are regions near the center of the shelf, and closer to the grounding line where the correlation switches sign, implying an increase in buttressing (as calculated in that direction) accompanying an increase in GLF (Fig. 8~~b). c~~).

~~Carrying this analysis one step further,~~ In addition to the results for the three discrete normal directions discussed above, a continuous analysis of $\Upsilon_{\rm gl}$ as a function of the normal stress direction is shown in Fig. 9 where we plot $\Upsilon_{\rm gl}$ ~~for~~ at each perturbation point ~~(span along the y axis)~~ and for *all* directions ~~(span along the x axis)~~ in the range of $\Delta\phi = 0$–180° relative to $\mathbf{n}_{p1}$. ~~Again, this~~ This correlation is generally negative and ~~substantially~~ stronger for buttressing numbers calculated ~~close to~~ near the $\mathbf{n}_{p1}$ direction (~~i.e., for~~ $\Delta\phi$ closer to 0° or 180°) and weaker (or even strongly positive) approaching the $\mathbf{n}_{p2}$ direction. This analysis connects the local perturbations and far-field impacts described above with changes in integrated GLF, providing a further means for understanding the correlation between $N_b(\mathbf{n}_{p1})$ and N_{rp} in Fig. 4b.

4.3.4 ~~Local~~ Summary of local versus integrated impacts of ~~changes in buttressing~~ice shelf perturbations

The changes in ice speed and buttressing at the grounding line ~~that are~~ quantified by Figs. 8 and 9 must be the result of perturbations initiated on the ice shelf that have propagated (here, instantaneously) to the grounding line, where increases in speed are associated with increased extension along $\mathbf{n}_{p1}$ and, according to Eq.~~(10)~~ (10), decreased buttressing associated with the $\mathbf{n}_{p1}$ direction. Intuitively, these increases in ice speed at the grounding line must be triggered by the loss of buttressing on the shelf~~. However, as discussed in the previous section, local perturbations and changes in buttressing on the shelf – as quantified by the changes in buttressing number calculated in all directions – are clearly not representative of the integrated changes in buttressing that are "felt" upstream at the grounding line (i.e., local increases in buttressing~~, initiated here via small and highly localized ice thickness (thinning) perturbations. As shown and argued above, however, it is difficult to understand the integrated impacts of these perturbations on ~~the shelf versus decreases in buttressing at the grounding line). This casts doubt on the utility of assessing the GLF sensitivity using locally derived buttressing numbers on the ice shelf (a discussion we return to below). The~~ GLF based on changes in locally derived quantities alone, in particular, the locally derived buttressing number, N_b. One would come to very different conclusions regarding how a perturbation impacts local buttressing depending on both the spatial scale of the area around a perturbation being examined and the principal direction used for calculating N_b (e.g., Figs. 7a and b). Over wider spatial scales, however, we do find consistency between the impacts of local perturbations on geometry, stresses, local buttressing, ice speed, and changes in GLF (Figs. 6, 8, 9). While we hypothesize that it is this consistency that lies behind the apparent correlation between ~~N_{rp} and $N_b(\mathbf{n}_{p1})$ (N_b~~ and N_{rp} in Fig. 4b~~) may be partially explained by Figs. 8a and 9, which suggests that $\mathbf{n}_{p1}$ may be the dominant direction controlling the ice flux across the grounding line for the MISMIP+ domain. In~~, we still lack the detailed physical understanding behind that correlation that would be required for us to apply it with confidence.

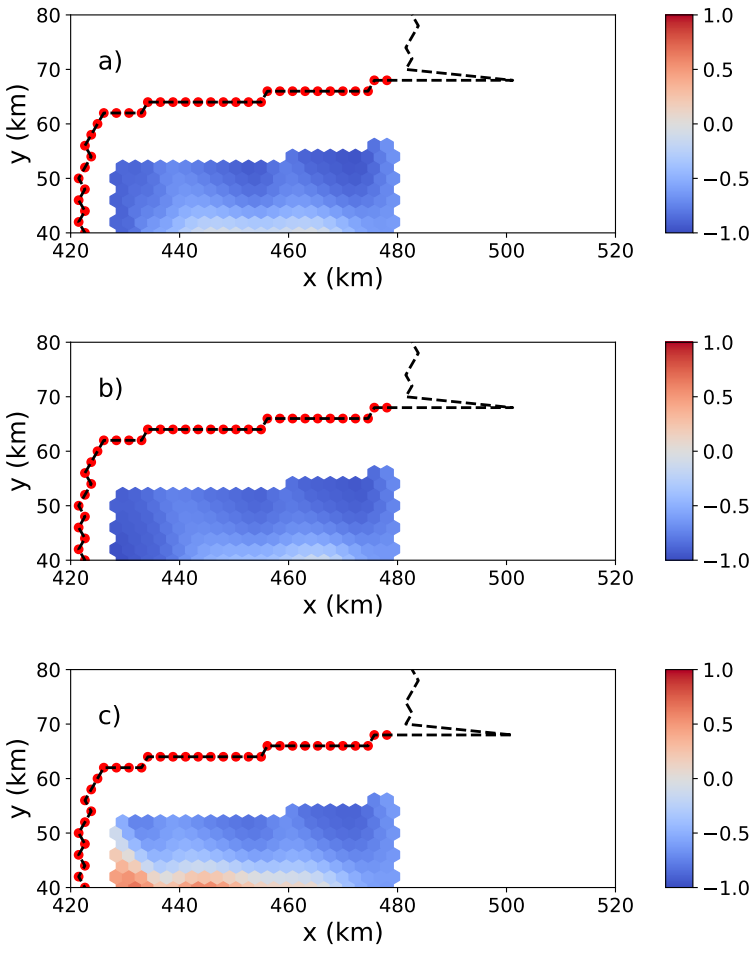

Figure 8. Spatial distribution of the correlation coefficient Υ_{gl} from Eq. ~~(13)~~ (13) over the MISMIP+ domain for buttressing number changes calculated parallel to (a) $\mathbf{n}_{gl}$, (b) $\mathbf{n}_{p1}$ and (~~b~~c) $\mathbf{n}_{p2}$ (colors). Υ_{gl} is a measure of the correlation between changes in buttressing number and ice speed along the grounding line. The black-dashed line represents the grounding line ~~, along~~ and the red dots indicate the area of the grounding line for which values of Υ_{gl} are calculated for each perturbation on the ice shelf, as shown in Fig. 4a.

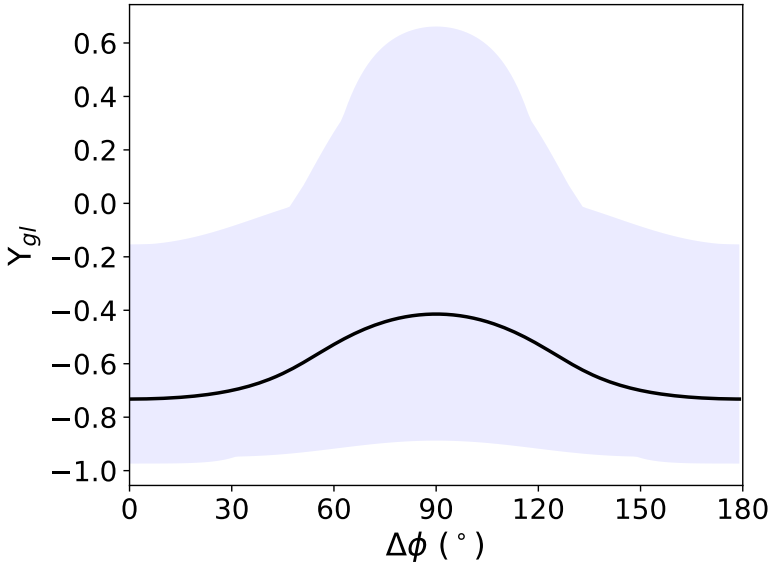

Figure 9. Correlation between the change in buttressing number and the change in ice speed across the grounding line (i.e., Υ_{gl} from Eq. ~~(13)~~(13)) for the entire MISMIP+ grounding line. The horizontal axis shows how Υ_{gl} varies as a function of the direction $\mathbf{n}$ used to define the normal stress, rotated counterclockwise from $\mathbf{n}_{p1}$ by $\Delta\phi$. Values from the maps in Figs. 8a and b plot at $\Delta\phi$ values of 0 and 90 degrees, respectively. Thus, the blue shaded region represents all possible maps for all possible values of buttressing direction. The thick black curve represents the mean value of Υ_{gl} for any given map.

Further, we show in the Supplementary Material and Table S01 that the correlation between may be spurious, perhaps due to correlations with some other common variable. Finally, in the next section ~~, we apply a similar set of analyses~~ we show that this tenuous correlation between N_b and N_{rp} breaks down almost entirely when applied to a realistic ice shelf~~and in doing so, demonstrate that these same correlations, already tenuous, are much more difficult to extract and interpret for realistic domains~~.

4.4 Application to Larsen C Ice Shelf

~~To explore whether the correlations between modeled and predicted N_{rp} found~~ We apply a similar set of analyses, as discussed above for the MISMIP+ ~~test case hold for realistic ice shelves, we apply a similar analysis to the Larsen C domain. In this case, the computational mesh resolution varies, from finer near the grounding line (2 km) to coarser towards the center of the ice shelf and calving front (4 km). In order to be comparable to the experiments and results of Reese et al. (2018), we use (approximately) 20 km × 20 km boxes for the application of ice-thickness perturbations, where the number of grid cells contained within each perturbation "box" is adjusted to sum to their correct total area~~[1]~~. Additionally, to investigate the impacts of the complex geometry of the Larsen C Ice Shelf (i.e., the grounding line shape, the existence of ice rises, etc.), we perform~~

[1] ~~We note that the actually area may vary slightly from 400 km^2 depending on the number and area of the variable resolution grid cells that are included in each perturbation "box".~~

two sets of perturbation experiments for which the 20 km × 20 km averaging boxes either do or do not include perturbations applied to cells near the grounding line.

Analogous to Fig. 5a domain, to a realistic, Larsen C ice shelf domain. For this domain, with complex geometry and spatially variable ice temperature (and associated ice rigidity), the relationship between $N_b(\mathbf{n}_{p1})$ and N_{xp} becomes much weaker relative to that for the MISMIP+ test case, Fig. **??**b shows domain. Fig. 10 shows that using the N_{rp}:N_b correlations for the Larsen C model domain (including only perturbation points that are >50 km away from both the calving front and grounding line). As found previously, calculating N_b using T_{nn} along $\mathbf{n}_{p1}$ provides a good overall correlation between N_b and N_{rp} shear metric m_s (Eq. ($\Delta\phi = 0°$ or $180°$) while calculating N_b using T_{nn} along $\mathbf{n}_{p2}$ provides the worst overall correlation ($\Delta\phi = 90°$).

In Fig. **??** we redo the same analysis but for points nearer to the grounding line (including points that are more than 20 km away from the calving front and the grounding line). This changes the values of r and also the relationship between the correlation coefficient and the alignment relative to $\mathbf{n}_{p1}$; the direction aligned with $\mathbf{n}_{p2}$ still gives the worst **??**)) to filter locations reduces the scatter between $N_b(\mathbf{n}_{p1})$ and N_{rp}:N_b correlation but the direction aligned with $\mathbf{n}_{p1}$ no longer gives the best correlation. This indicates that thickness perturbations at these locations are propagating in a more complex way on a real ice shelf, especially for perturbation points that are close to the grounding line. We expect that the correlations would further degrade as additional perturbation points closer to grounding line are included in the analysis.

(a) The locations of the 20 km × 20 km perturbation boxes (15, solid blue dots). The red and black dotted lines are the grounding line and the boundary of model domain, respectively. (b) The N_{rp} : N_b correlation coefficients for each direction rotated counterclockwise from the direction of $\mathbf{n}_{p1}$ (as in Figure 5a but for the Larsen C domain).

(a) The locations of the 20 km × 20 km perturbation boxes (solid blue dots). The red and black dotted lines are the grounding line and the boundary of model domain, respectively. (b) The N_{rp} : N_b correlation coefficients for each direction rotated counterclockwise from the direction of $\mathbf{n}_{p1}$ (as in Figure **??**b but including additional analysis points closer to the grounding line and calving front).

In the supplement, we include figures showing the . However, even when retaining only points with low shear contributions, the relationship is nonlinear without a clear functional form. Furthermore, restricting analysis to the maximum and minimum ice speed increases in the vicinity of perturbation cells, local changes in geometry and buttressing, and the correlations between the changes of buttressing number and ice speed on the ice shelf and along the grounding line (i.e., figures analogous to Figs. **??**, 6, 7 and 9 but for the Larsen C domain instead). As for the MISMIP+ domain, low shear regions where the relationship is stronger excludes the majority of the ice shelf, including most of the directions of maximum ice speed increase for Larsen C are also aligned closely with the ice flow direction (Fig. **??**). Similarly, we find that the ice speed increase following thickness perturbations on the Larsen C shelf increase buttressing locally regions of where the GLF response number is large (see also Fig. 13a below). We find a similar result when coarsening the analysis to use 20 × 20 km boxes for the analysis, as was done for the N_{xp} calculations performed by Reese et al. (2018); a strong correlation exists for only a small area near the center of the ice shelf (Fig. **??**, **??**). We do not, however, find any clear correlation between changes in buttressing number and ice speed along the grounding line for Larsen C (Fig. **??**). S6). Even weaker relationships are found for the $\mathbf{n}_{p2}$ and $\mathbf{n}_f$ directions. Thus,

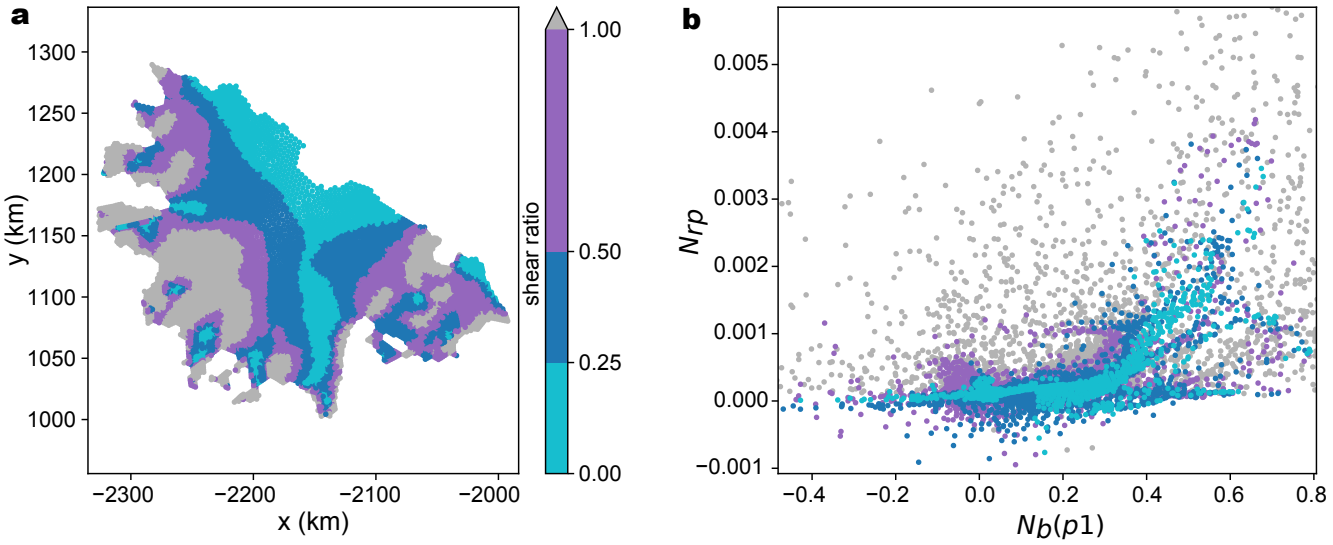

Figure 10. a) Larsen C model domain colored by the shear metric, m_s (Eq. (??)). b) Scatter plot of $N_b(p1)$ and N_{rp} colored by different values of m_s.

while there clearly is some link between $N_b(\mathbf{n}_{p1})$ and N_{rp} for a realistic ice shelf, it is far too tenuous to be used in a predictive way and likely differs across and between ice shelves.

Overall, for a realistic ice shelf like Larsen C with a complex geometry and flow field, ~~it is difficult to find the robust , directionally dependent relationships seen for the more idealized, MISMIP+ domain~~we find it even more difficult to demonstrate robust relationships between the local ice shelf buttressing number and changes in GLF. This is~~likely because~~, at least in part, likely due to the fact that, for more complex and realistic domains, there is no dominant direction of buttressing controlling ice flux across the grounding line. ~~This finding further diminishes~~ These findings further diminish our confidence in ~~attempting to use a simple metric like a locally derived ice shelf buttressing number~~using locally derived buttressing numbers for assessing the sensitivity of GLF to changes on the ice shelf. For this reason, we ~~now~~ explore an alternative and more robust method for quantifying how ice shelf thickness perturbations affect flux at the grounding line.

4.5 Adjoint sensitivity

~~Our~~ While our goal throughout this study has been to find a simple and robust metric for diagnosing GLF sensitivity to ice shelf thickness perturbations~~. However, the~~ , the challenges and complications discussed above suggest that this may not be possible~~, motivating~~ . This motivates our investigation of a wholly different approach~~.~~ , which ~~This approach~~ provides a GLF sensitivity map analogous to that ~~provided by the Reese et al. (2018)finite perturbation-based experiments (and those conducted here)~~from Reese et al. (2018). But rather than computing the GLF change due to a perturbation applied individually at each of n model grid cells (thus requiring n diagnostic solves), we use an adjoint-based method that allows for the computation of the

sensitivity at all n grid cells simultaneously ~~for~~ at the cost of a single adjoint-model solution. Briefly, this method involves the solution of an auxiliary linear system (the adjoint system) to compute the so-called Lagrange multiplier, a variable with the same dimensions as the forward-model solution for the ice velocity. Here, the matrix associated with the system is the transpose of the Jacobian of the first-order approximation to the Stokes flow model (Perego et al., 2012). In addition, the adjoint method requires computation of the partial derivatives of the first-order model residual and the GLF with respect to the velocity solution and the ice thickness. Here, we compute the Jacobian and all the necessary derivatives using automatic differentiation (Tezaur et al., 2015a). Additional details of the adjoint-based method and calculations are giving in Appendix ~~B~~C.

A similar approach has been proposed by Goldberg et al. (2019). That work primarily assessed the adjoint sensitivity of the volume above floatation with respect to sub-ice shelf melting of Dotson and Crosson ice shelves in West Antarctica. In contrast to our approach, Goldberg et al. (2019) compute *transient* sensitivities because their quantity of interest (volume above floatation) is time dependent.

The adjoint-based sensitivity has units of ~~mass~~ volume flux per year per meter of ice thickness perturbation (~~kg a^{-1} m~~m^2 yr^{-1}). We ~~normalize this valueby the mass change per year due to the thickness perturbation~~nondimensionalize this value, dividing it by the area of the perturbed cell and multiplying it by the one year period over which we consider the perturbation, so that it is dimensionless and comparable to N_{rp}, and refer to it as N_{ra} (where the subscript a is for "adjoint"). In Figs. 11 and 12, we demonstrate the application of this method to the MISMIP+ and Larsen C domains by comparing GLF sensitivities deduced from 730 and 1000 ~~individual diagnostic model evaluations~~ points (i.e., from the respective perturbation experiments discussed above [1]for the MISMIP+ and Larsen C domains, respectively) with those deduced from a single adjoint-based solution~~. Note that for some cells adjacent to the grounding line, the negative sensitivity values may be caused by partially grounded cells (i.e., a thinning of ice thickness there may induce a decrease in ice flux across the grounding line). The comparison in Figs. 11 and 12~~ . The comparison demonstrates that the two approaches provide a near exact match.

As might be expected based on the discussion above, the two methods disagree in regions very near to the grounding line (see Fig. 13c). This discrepancy is likely a consequence of ~~the high~~ large non-linearities near the grounding line, as suggested by the fact that the agreement between the two methods improves as the size of the perturbation decreases (from 10 m to 0.001 m; see Fig. 13), the only change being the magnitude of the applied perturbation). This might be exacerbated by the sliding law adopted in this work, which results in abrupt changes in the basal traction across the grounding line~~(other sliding lawsallowing~~ . Other sliding laws, e.g. Brondex et al. (2017), allow for a smoother transition at the grounding line ~~, e.g. Brondex et al. (2017),~~ and might mitigate this problem. We also note that some isolated cells adjacent to the grounding line exhibit negative sensitivities (a *decrease* in ice flux following a *decrease* in ice thickness), opposite those exhibited by the rest of the ice shelf. We attribute these to partially grounded cells, for which the sensitivity may be more akin to that expected for grounded ice (i.e., a direct relationship between ice thickness and ice flux).

The adjoint sensitivity map represents a linearization of the GLF response to thickness perturbations. As long as the perturbations are small enough, one can approximate the GLF response by multiplying the sensitivity map by the thickness perturbation. Comparison of N_{ra} and N_{rp} for different perturbation sizes (Fig. 13) suggests that this is reasonable for perturbations on the

[1]~~For Larsen C, we conduct perturbation experiments at individual grid cells to allow for a closer comparison with the adjoint method.~~

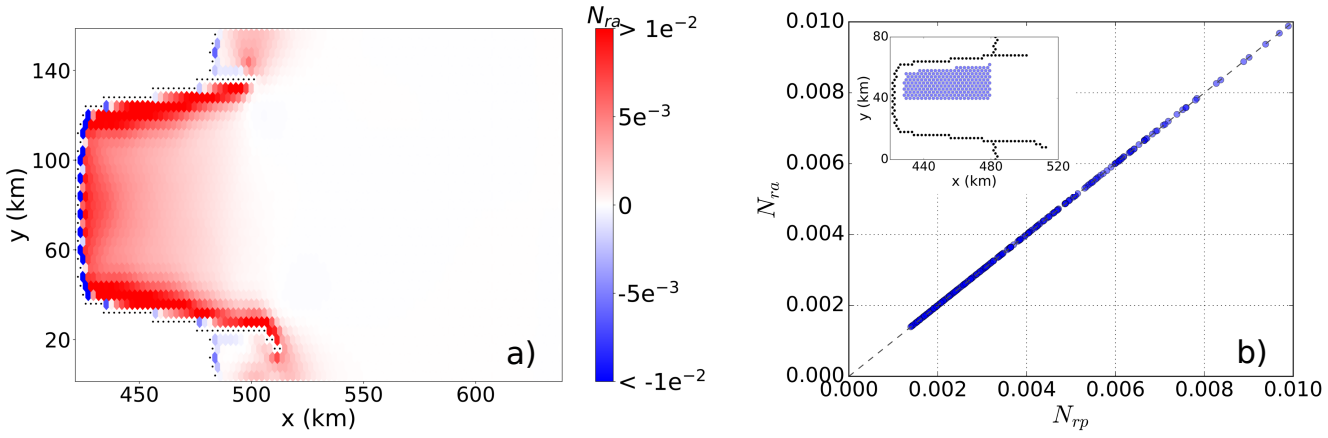

Figure 11. (a) Grounding line flux sensitivity for the MISMIP+ domain derived from the ~~an~~ adjoint model approach~~;~~. (b) Perturbation- (N_{rp}; x-axis) versus adjoint-based (N_{ra}; y-axis) sensitivies ~~are~~ plotted against one another (perturbation locations are shown by circles in the inset, where the grounding line grid cells are shown by the black dots.)

order of $<$10 m for points on the ice shelf that are not too close to the GL. At the same time care should be taken when interpreting the sensitivities – based on either the perturbation- or adjoint-based methods – in the vicinity of grounding lines. This is especially important when considering that the near-grounding-line region is also that with the largest sensitivities (Figs. 11a and 12a). Because these sensitivities may be inaccurate, they provide an ~~additional~~ argument for applying high spatial resolution near the grounding line; coarse resolution near the grounding line will extend the region over which inaccurate ~~sensitivites~~ sensitivities may be assessed. More accurately assessing the sensitivities near the grounding line may require the application of perturbations ~~more realistic in both magnitude and spatial scale, as opposed to~~ with both magnitudes and spatial scales that are more realistic than the infinitesimal, highly localized perturbations explored here.

The ~~adjoint-method~~ adjoint method provides sensitivity maps over the entire ice shelf, including around islands, promontories, and along the grounding line itself, which is generally the part of the ice shelf where the GLF is the most sensitive to thickness perturbations (e.g., see Figs. 11a and 12a ~~above~~ and Fig. 1 in ~~Reese et al. (2018)~~Reese et al. 2018). Thus, despite the added complexity in its computation, the adjoint-based method provides significant advantages over the simpler but more *ad hoc* (i.e., perturbation-based) analysis methods discussed above.

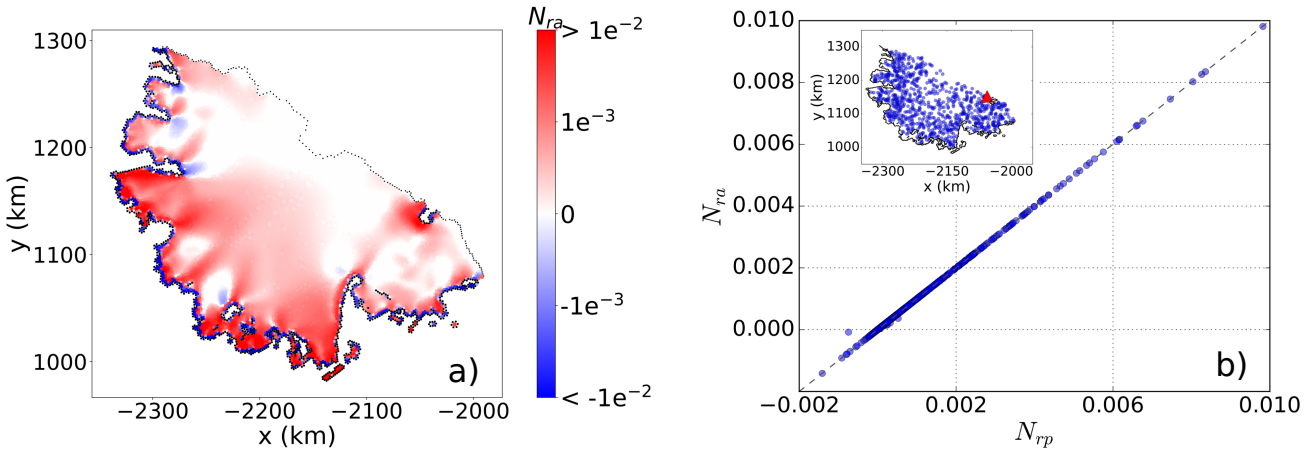

Figure 12. (a) Grounding line flux sensitivity for the Larsen C domain derived from the adjoint model approach~~;~~ . (b) Perturbation- (N_{rp}; x-axis) versus adjoint-based (N_{ra}; y-axis) sensitivies ~~are~~ plotted against one another (perturbation locations are shown by circles in the inset, where the one outlier in b) is at the calving front (red triangle), and the grounding line in is shown by the black curve.)

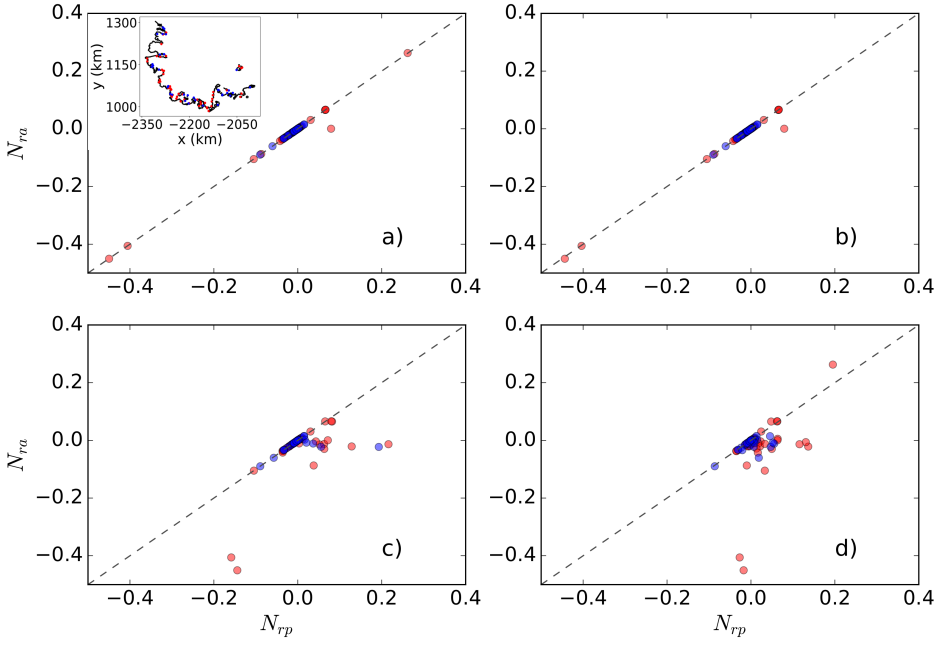

Figure 13. Comparisons between perturbation- and adjoint-based sensitivities (N_{rp} and N_{ra}, respectively) for ice thickness perturbation of (a) 0.001 m, (b) 0.01 m, (c) 1 m and (d) 10 m for perturbation points near the grounding line (<3 km) ~~, as shown as~~ indicated by the ~~red solid circles in~~ dots on the inset map in (a). Red dots represent grid cells next to the grounding line and blue dots represent grid cells on the ice shelf proper.

5 Discussion and Conclusions

The current interest in better understanding the controls on the MISI is due to the potential for future (and possibly present-day, ongoing) unstable retreat of the West Antarctic ice sheet (e.g., Joughin et al., 2014; Hulbe, 2017; Konrad et al., 2018). Because a loss of ice shelf buttressing is a primary cause of increased GLF (and thus an indirect control on the MISI), recent attention has focused on better understanding the sensitivity of ice shelf buttressing to increases in iceberg calving and sub-ice shelf melting. In this study, we have attempted to better characterize and quantify how local thickness perturbations on ice shelves – a proxy for local thinning due to increased sub-ice shelf melting – impact ice shelf buttressing and GLF.

~~Two previously used~~ Two previous approaches for assessing GLF sensitivity to changes in ice shelf buttressing – the flux response number (N_{rp}) and the buttressing number (N_b) – ~~are reasonably well correlated in some situations. This correlation is , however,~~ only show significant correlations with one another only over regions with a relatively small shear component. In addition, this correlation is highly dependent on the direction chosen to define buttressing. Specifically, we find that the choice of the normal vector used when calculating N_b dictates whether ~~there is a general correlation or lack of~~ the correlation between N_{rp} and N_b is significant or not. Here, for both idealized and realistic ice shelf domains, we find a ~~stronger~~ weak correlation between N_{rp} and N_b when the normal stress used in calculating the buttressing number corresponds to the ~~first principal stress or the ice flow direction , whereas the correlation is much weaker~~ second principal stress direction ($\mathbf{n}_{p2}$). The correlation is stronger (though sometimes still fairly weak) when N_b is calculated in the direction associated with the ~~second principal stress .~~ first principal stress ($\mathbf{n}_{p1}$) or the ice flow ($\mathbf{n}_f$).

These findings appear at odds with the interpretation from previous efforts of ~~Fürst et al. (2016)~~Fürst et al. (2016), who argue that buttressing provided by an ice shelf is best quantified by N_b calculated in the direction of $\mathbf{n}_{p2}$. ~~These seemingly contradictory findings~~ The seeming contradiction may be partially rectified by considering the different foci of Fürst et al. (2016) versus the present work: while Fürst et al. (2016) primarily focused on how the removal of passive shelf ice (identified by $N_b(\mathbf{n}_{p2})$) impacted ice shelf dynamics, as quantified by the *change in ice flux across the calving front*, our focus is specifically on how localized ice shelf thickness perturbations impact the *change in ice flux across the grounding line*[1]. While changes in calving flux are likely to impact the amount of buttressing provided by an ice shelf, they do not directly contribute to changes in sea level. For this reason, changes in GLF are arguably the more important metric to consider when assessing the impacts of changes in ice shelf buttressing.

Of significant concern in applying the apparent correlation between N_{rp} and N_b (relatively difficult and easy quantities to calculate, respectively) ~~to diagnose N_{rp} from observations or models~~ is the lack of a clear physical connection between local changes in buttressing on the ice shelf and integrated changes in flux at the grounding line. Here, we show that localized thinning on the shelf ~~generally leads to a local~~ can lead to either increases ~~*increasein*~~ *or* decreases in the local buttressing metric N_b, depending on both the direction of the normal stress chosen and the neighborhood over which these changes are estimated. Yet these same perturbations consistently result in a net *decrease* in buttressing and ~~an~~ consequently a net *increase* in ~~ice flux~~

[1]While Fürst et al. (2016) also discuss the impact of perturbations on the flux across the grounding line, this is a secondary focus of their paper and mostly discussed in the Supplementary ~~Information~~Material.

~~across the grounding line . This~~ grounding line flux. While this can often be understood through the detailed spatial analysis of the impacts for a single perturbation (e.g., Section 4.3 and Fig.6), this finding suggests that local evaluations of buttressing on the ice shelf ~~need to~~ alone should be interpreted with extreme caution, as they may not be physically meaningful with respect to understanding ~~and quantifying~~ overall changes in GLF. It is also possible that the correlations we find between N_{rp} and N_b are ~~simply fortuitous , and thus not meaningful in any physical way~~ [2]. fortuitous or spurious, giving us further pause in attempting to apply them in a predictive sense.

Practically speaking, however, these ~~distinctions and concerns~~ nuances may be irrelevant; when realistic ~~,~~ and complex ice shelf geometries are considered, ~~it is not possible to define or even identify clear~~ clear and robust relationships between N_{rp} and N_b are elusive or absent. For the Larsen C domain considered here, strong, positive correlations are only found to exist over a small, isolated region near the center of the ice shelf~~. Proximity~~ ; proximity to the grounding line, the calving front, complex coastlines, islands, and promontories all serve to degrade these correlations significantly, reducing the utility of the buttressing number as a simple metric for diagnosing GLF sensitivity on real ice shelves. Further, defining "proximity", and hence an adequate distance away from these complicating features or other filtering metric, appears to be largely arbitrary. Lastly, it is precisely these more complex regions, close to the ice shelf grounding lines, where sub-ice shelf thinning will result in the largest impact on changes in GLF (as demonstrated ~~here~~ in Figs. 11a and 12a).

Considering these complexities, we propose that assessing GLF sensitivities for real ice shelves requires an approach ~~much more~~ analogous to the perturbation method used by Reese et al. (2018). Due to the computational costs and the experimental design complexity associated with the perturbation-based method we propose that an adjoint-based method is the more efficient way for assessing GLF sensitivity to changes in buttressing resulting from changes in sub-ice shelf melting. Future work should focus on applying these methods to assessing the sensitivities of real ice shelves, based on observed or modeled patterns of sub-ice shelf melting, and assessing how these sensitivities change in time along with the evolution of the coupled ocean-and-ice shelf system.

6 Acknowledgements

The authors thank Hilmar Gudmundsson, two anonymous reviewers, and the editor, Olivier Gagliardini, for comments and suggestions that significantly improved the manuscript. Support for this work was provided through the Scientific Discovery through Advanced Computing (SciDAC) program funded by the U.S. Department of Energy (DOE) Office of Science, Biological and Environmental Research and Advanced Scientific Computing Research programs. This research used resources of the National Energy Research Scientific Computing Center, a DOE Office of Science user facility supported by the Office of Science of the U.S. Department of Energy under Contract DE-AC02-05CH11231, and resources provided by the Los Alamos

[2] ~~We note that the correlations we discuss here, between N_{rp}, $N_b(\mathbf{n}_f)$, and $N_b(\mathbf{n}_{p1})$ were alluded to in the Supplement from Fürst et al. (2016), where they note that "Outside the Passive Shelf Icearea, melting will affect the buttressing potential. Consequences for upstream tributary glaciers are then best estimated from buttressing in the flow direction."~~

National Laboratory Institutional Computing Program, which is supported by the U.S. Department of Energy National Nuclear Security Administration under Contract DE-AC52-06NA25396.

7 Code and data availability

The code of the ice sheet model (MALI) can be found here: https://github.com/MPAS-Dev/MPAS-Model/releases (V6.0). The datasets used in this paper can be found in https://doi.org/10.5281/zenodo.3872586.

8 Author contribution

Tong Zhang and Stephen Price initiated the study with input from Matthew Hoffman, Mauro Perego, and Xylar Asay-Davis. Tong Zhang conducted the diagnostic simulations with MALI and the majority of the analysis. The adjoint experiments were conducted by Mauro Perego. ~~Tong Zhang conducted the diagnostic simulations with MALI. Tong Zhang and Stephen Price wrote the paperwith contributions from all co-authors~~All authors contributed to the writing of the paper.

9 Competing interests

The authors declare that they have no conflict of interest.

Appendix A: Calculation of the buttressing number

At the calving front, the stress balance is given by,

$$\sigma \cdot \mathbf{n} = -p_w \mathbf{n}, \tag{A1}$$

where σ is the Cauchy stress tensor, $\mathbf{n}$ is the unit normal vector pointing horizontally away from the calving front, and p_w is the ~~sea water pressure~~ water pressure against the calving front provide by the ocean. In a Cartesian reference frame, this gives two equations for the stress balance in the two horizontal directions,

$$\begin{aligned} \sigma_{xx} n_x + \sigma_{xy} n_y &= -p_w n_x, \\ \sigma_{xy} n_x + \sigma_{yy} n_y &= -p_w n_y. \end{aligned} \tag{A2}$$

Expressing the ~~full~~ Cauchy stress as the sum of the deviatoric stress and the isotropic pressure (~~$\sigma = \tau - p$~~$\sigma = \tau - pI$) and assuming that the vertical normal stress σ_{zz} is hydrostatic gives,

$$p = \rho_i g(s - z) - \tau_{xx} - \tau_{yy}. \tag{A3}$$

Combining Equations A2 and A3 gives,

$$\begin{aligned} (2\tau_{xx} + \tau_{yy}) n_x + \tau_{xy} n_y &= -p_w n_x + \rho_i g(s - z) n_x, \\ \tau_{xy} n_x + (2\tau_{yy} + \tau_{xx}) n_y &= -p_w n_y + \rho_i g(s - z) n_y. \end{aligned} \tag{A4}$$

~~By vertically integrating Equation A4 and approximating the depth-integrated viscosity as $\overline{\mu} = \mu H$, we obtain~~ On ice shelves, the left hand terms in Equations A4 can be taken as invariant in the z direction and by vertically averaging A4 we obtain

$$(2\tau_{xx} + \tau_{yy})n_x + \tau_{xy}n_y = \frac{1}{2}\rho_i g(1 - \frac{\rho}{\rho_w})Hn_x,$$
$$\tau_{xy}n_x + (2\tau_{yy} + \tau_{xx})n_y = \frac{1}{2}\rho_i g(1 - \frac{\rho}{\rho_w})Hn_y. \quad \text{(A5)}$$

If we define the two-dimensional stress tensor $\mathbf{T}$ as,

$$\mathbf{T} = \begin{pmatrix} 2\tau_{xx} + \tau_{yy} & \tau_{xy} \\ \tau_{xy} & 2\tau_{yy} + \tau_{xx} \end{pmatrix}, \textit{thenwewillhave} \textit{wecanwriteEq.} \text{ (A5)} \textit{as} \mathbf{Tn} = N_0\mathbf{n}, \quad \text{(A6)}$$

where $N_0 = \frac{1}{2}\rho_i g(1 - \rho_i/\rho_w)H$ is the average pressure exerted by the ocean against the calving front (as defined in Eq. (11)). The buttressing number, defined by

$$N_b = 1 - \frac{\mathbf{n} \cdot \mathbf{Tn}}{N_0}, \quad \text{(A7)}$$

is thus a scalar measure of the balance between this average ocean pressure and internal stress within the ice shelf. For the case of $N_b = 0$, these two exactly balance such that stresses within the ice shelf do not further restrain or compel the ice flow.

Appendix B: Relationship between buttressing number and backstress

Thomas (1979) defines the concept of "back-pressure" or "back stress", which was formalized by Thomas and MacAyeal (1982) and MacAyeal (1987) as the stress provided by lateral shearing and compression around ice rises in excess of that of a freely spreading ice shelf. While the concept was conceived as applying along the grounding line (Thomas, 1979; MacAyeal, 1987), it was extended to any material surface within an ice shelf (Thomas and MacAyeal, 1982; MacAyeal, 1987). This older concept of a normal pressure characterizing downstream ice shelf conditions is reminiscent of the buttressing number defined by Gudmundsson (2013) and extended by Fürst et al. (2016) as the buttressing number (N_b)~~as~~, defined in Eq. (A7) (and Eq. (10)). Here we show that backstress is equivalent to N_b calculated in the along flow direction and normalized by the hydrostatic stress.

We follow Van Der Veen (2013) and Cuffey and Paterson (2010) and define back force, F_B, as the difference between the driving force of an ice shelf, F_D and the resistive force from longitudinal stretching, F_L:

The driving force for an ice shelf is

$$F_D = \frac{1}{2}\rho_i g(1 - \frac{\rho_i}{\rho_w})H^2, \quad \text{(B1)}$$

and the longitudinal stretching force for a freely spreading ice shelf is

$$F_L = H(2\tau_{xx}^f + \tau_{yy}^f), \quad \text{(B2)}$$

where τ^f_{xx} and τ^f_{yy} are the along-flow and across-flow deviatoric stresses, respectively.

$$N_0 F_L = \frac{1}{2}\rho_i g(1 - \frac{\rho_i}{\rho_w}) H . T^f_{xx}, \tag{B3}$$

according to Eq. (A6), where T^f_{xx} is the along-flow stress in the along-flow coordinate system, equivalent to the normal stress along the flow direction, $\mathbf{n}_f \cdot \mathbf{T}\mathbf{n}_f$, in the x, y coordinate system. To obtain the backstress, B_s, as a stress normal to a vertically-oriented material surface, divide Eq. (**??**) by thickness (force per unit width divided by thickness):

$$B_s = \frac{F_B}{H} = \frac{F_D}{H} - \frac{F_L}{H}. \tag{B4}$$

However, if we observe that the driving stress of an ice shelf is the hydrostatic stress, N_0 (Eq. (11)), multiplied by the thickness,

$$F_D = N_0 H, \tag{B5}$$

combined with Eq. (B3), we can rewrite the backstress as

$$B_s = N_0 - \mathbf{n}_f \cdot \mathbf{T}\mathbf{n}_f. \tag{B6}$$

Dividing (normalizing) by N_0 then gives

$$\frac{B_s}{N_0} = 1 - \frac{\mathbf{n}_f \cdot \mathbf{T}\mathbf{n}_f}{N_0} = N_b(\mathbf{n}_f), \tag{B7}$$

which is analogous to Eq. (A7) above.

This result, while fairly straightforward to arrive at, brings together the current concept of "buttressing" at the grounding line (as defined by Gudmundsson (2013) and extended to buttressing number on the ice shelf by Fürst et al. (2016)), with the much older concept of ice shelf "backstress" (e.g., Thomas and MacAyeal, 1982).

Appendix C: Adjoint calculation of GLF sensitivity

The adjoint method is often used to compute the derivative (or "sensitivity") of some quantity (here, the GLF) that depends on the solution of a partial differential equation, with respect to parameters (here, the ice thickness) (see, e.g., Gunzburger (2012)). It is particularly effective when the number of parameters is large because it only requires the solution of an additional linear system, independent of the number of parameters. In the discrete case, the GLF is a function of the ice speed vector, $\mathbf{u}$, and the ice thickness vector, $\mathbf{H}$. Using the chain rule, we compute the total derivative of the GLF with respect to the ice thickness as:

$$\frac{d(\text{GLF})}{d\mathbf{H}} = \frac{\partial(\text{GLF})}{\partial \mathbf{u}} \frac{\partial \mathbf{u}}{\partial \mathbf{H}} + \frac{\partial(\text{GLF})}{\partial \mathbf{H}}. \tag{C1}$$

Here $\frac{\partial \mathbf{u}}{\partial \mathbf{H}}$ denotes the matrix with components $\left(\frac{\partial \mathbf{u}}{\partial \mathbf{H}}\right)_{ij} = \frac{\partial \mathbf{u}_i}{\partial \mathbf{H}_j}$. Similarly $\frac{\partial(\text{GLF})}{\partial \mathbf{u}}$ and $\frac{\partial(\text{GLF})}{\partial \mathbf{H}}$ are row vectors with components $\frac{\partial(\text{GLF})}{\partial \mathbf{u}_j}$ and $\frac{\partial(\text{GLF})}{\partial \mathbf{H}_j}$ ~~repsectively. In~~ respectively. The first term on the right-hand side of Eq. (C1) accounts for the

fact that a perturbation of the thickness would affect the ice velocity, which in turn would affect the GLF. The second term on the right-hand side of Eq. (C1) accounts for changes in the GLF directly due to changes in thickness and is non-zero only when the thickness is perturbed at triangles intersecting the GL. In this case, a thickness perturbation would affect the position/length of the GL and the thickness of the ice at the GL.

In order to compute $\frac{\partial \mathbf{u}}{\partial \mathbf{H}}$, we write the finite element discretization (Tezaur et al. (2015b)) of the flow model (Eq. (1)) in the residual form $\mathbf{c}(\mathbf{u}, \mathbf{H}) = \mathbf{0}$ and differentiate with respect to $\mathbf{H}$:

$$\mathbf{0} = \frac{d\mathbf{c}}{d\mathbf{H}} = \frac{\partial \mathbf{c}}{\partial \mathbf{u}} \frac{\partial \mathbf{u}}{\partial \mathbf{H}} + \frac{\partial \mathbf{c}}{\partial \mathbf{H}}. \tag{C2}$$

Here $J := \frac{\partial \mathbf{c}}{\partial \mathbf{u}}$ is a square matrix referred to as the Jacobian. It follows that $\frac{\partial \mathbf{u}}{\partial \mathbf{H}}$ is solution of

$$J \frac{\partial \mathbf{u}}{\partial \mathbf{H}} = -\frac{\partial \mathbf{c}}{\partial \mathbf{H}}. \tag{C3}$$

Note that this corresponds to solving many linear systems, one for each column of $\frac{\partial \mathbf{u}}{\partial \mathbf{H}}$ (i.e. for each entry of the ice thickness vector). We can then compute the sensitivity as

$$\frac{d(\text{GLF})}{d\mathbf{H}} = -\frac{\partial(\text{GLF})}{\partial \mathbf{u}} \left(J^{-1} \frac{\partial \mathbf{c}}{\partial \mathbf{H}} \right) + \frac{\partial(\text{GLF})}{\partial \mathbf{H}}. \tag{C4}$$

The main idea of the adjoint-based method is to introduce an auxiliary vector variable $\boldsymbol{\lambda}$ for solution of the *adjoint* system

$$J^T \boldsymbol{\lambda} = -\left(\frac{\partial(\text{GLF})}{\partial \mathbf{u}} \right)^T \tag{C5}$$

and then to compute the sensitivity as

$$\frac{d(\text{GLF})}{d\mathbf{H}} = \boldsymbol{\lambda}^T \frac{\partial \mathbf{c}}{\partial \mathbf{H}} + \frac{\partial(\text{GLF})}{\partial \mathbf{H}}. \tag{C6}$$

Equations (C4) and (C6) are equivalent, but the latter has the advantage of requiring the solution of a single linear system given by Equation (C5). In MALI, the Jacobian and the other derivatives, $\frac{\partial \mathbf{c}}{\partial \mathbf{H}}$, $\frac{\partial(\text{GLF})}{\partial \mathbf{u}}$, and $\frac{\partial(\text{GLF})}{\partial \mathbf{H}}$, are computed using automatic differentiation, a technique that allows for exact calculation of derivatives up to machine precision. For automatic-differentiation, MALI relies on the Trilinos *Sacado* package (Phipps and Pawlowski, 2012). As a final remark, we note that the term $\frac{\partial \mathbf{c}}{\partial \mathbf{H}}$ requires the computation of shape derivatives, because a change in thickness affects the geometry of the problem. This is not the case for two-dimensional, depth-integrated flow models (e.g., as in Goldberg et al. (2019)), or when using a sigma-coordinate to discretize the vertical dimension.

We conclude this section pointing out that the sensitivity $\frac{d(\text{GLF})}{d\mathbf{H}}$ depends on the local refinement of the mesh and it vanishes as the mesh is refined. This is particularly important in the case of nonuniform meshes, because the sensitivity map would strongly depend on the refinement. In order to overcome this issue it is advisable to scale the sensitivity pre-multiplying it by the inverse of the mass matrix (in a finite element context) or, similarly, dividing it point-wise by the measure (area) of the dual cells, as done in this paper to compute N_{ra}. We refer to Li et al. (2017), Section 6, for an in-depth analysis, in the optimization context.

References

Asay-Davis, X. S., Cornford, S. L., Durand, G., Galton-Fenzi, B. K., Gladstone, R. M., Gudmundsson, H., Hattermann, T., Holland, D. M., Holland, D., Holland, P. R., et al.: Experimental design for three interrelated marine ice sheet and ocean model intercomparison projects: MISMIP v. 3 (MISMIP+), ISOMIP v. 2 (ISOMIP+) and MISOMIP v. 1 (MISOMIP1), Geoscientific Model Development, 9, 2471–2497, 2016.

Bamber, J. L., Riva, R. E., Vermeersen, B. L., and Lebrocq, A. M.: Reassessment of the potential sea-level rise from a collapse of the west antarctic ice sheet, Science, 324, 901–903, https://doi.org/10.1126/science.1169335, www.sciencemag.org/cgi/content/full/324/5929/901, 2009.

Brondex, J., Gagliardini, O., Gillet-Chaulet, F., and Durand, G.: Sensitivity of grounding line dynamics to the choice of the friction law, Journal of Glaciology, 63, 854–866, 2017.

Cornford, S., Seroussi, H., Asay-Davis, X., Arthern, R., Borstad, C., Christmann, J., Dias dos Santos, T., Feldmann, J., Goldberg, D., Hoffman, M., Humbert, A., Kleiner, T., Leguy, G., Lipscomb, W., Merino, N., Durand, G., Morlighem, M., Polllard, D., Rückamp, M., and Yu, H.: Results of the third Marine Ice Sheet Model Intercomparison Project (MISMIP+), The Cryosphere Discussions, pp. 1–26, https://doi.org/10.5194/tc-2019-326, 2020.

Cornford, S. L., Martin, D. F., Payne, A. J., Ng, E. G., Le Brocq, A. M., Gladstone, R. M., Edwards, T. L., Shannon, S. R., Agosta, C., van den Broeke, M. R., Hellmer, H. H., Krinner, G., Ligtenberg, S. R. M., Timmermann, R., and Vaughan, D. G.: Century-scale simulations of the response of the West Antarctic Ice Sheet to a warming climate, The Cryosphere, 9, 1579–1600, https://doi.org/10.5194/tc-9-1579-2015, 2015.

Cuffey, K. and Paterson: The Physics of Glaciers, Butterworth-Heinneman, Amsterdam, 4th edn., 2010.

De Rydt, J., Gudmundsson, G., Rott, H., and Bamber, J.: Modeling the instantaneous response of glaciers after the collapse of the Larsen B Ice Shelf, Geophysical Research Letters, 42, 5355–5363, 2015.

Fretwell, P., Pritchard, H. D., Vaughan, D. G., Bamber, J., Barrand, N., Bell, R., Bianchi, C., Bingham, R., Blankenship, D., Casassa, G., et al.: Bedmap2: improved ice bed, surface and thickness datasets for Antarctica, The Cryosphere, 7, 375–393, https://doi.org/10.5194/tc-7-375-2013, 2013.

Fürst, J. J., Durand, G., Gillet-Chaulet, F., Tavard, L., Rankl, M., Braun, M., and Gagliardini, O.: The safety band of Antarctic ice shelves, Nature Climate Change, 6, 479, 2016.

Gagliardini, O., Durand, G., Zwinger, T., Hindmarsh, R., and Le Meur, E.: Coupling of ice-shelf melting and buttressing is a key process in ice-sheets dynamics, Geophysical Research Letters, 37, 2010.

Goldberg, D. N., Gourmelen, N., Kimura, S., Millan, R., and Snow, K.: How Accurately Should We Model Ice Shelf Melt Rates?, Geophysical Research Letters, 46, 189–199, https://doi.org/10.1029/2018GL080383, 2019.

Greve, R. and Blatter, H.: Dynamics of ice sheets and glaciers, Springer Science & Business Media, 2009.

Gudmundsson, G.: Ice-shelf buttressing and the stability of marine ice sheets, The Cryosphere, 7, 647–655, 2013.

Gudmundsson, G. H.: Transmission of basal variability to a glacier surface, Journal of Geophysical Research: Solid Earth, 108, 2003.

Gudmundsson, H., Krug, J., Durand, G., Favier, L., and Gagliardini, O.: The stability of grounding lines on retrograde slopes, The Cryosphere, 6, 1497–1505, 2012.

Gunzburger, M. D.: Perspectives in Flow Control and Optimization: Chapter 2. Three Approaches to Optimal Control and Optimization, Siam, https://doi.org/10.1137/1.9780898718720.ch2, 2012.

Hoffman, M. J., Perego, M., Price, S. F., Lipscomb, W. H., Zhang, T., Jacobsen, D., Tezaur, I., Salinger, A. G., Tuminaro, R., and Bertagna, L.: MPAS-Albany Land Ice (MALI): a variable-resolution ice sheet model for Earth system modeling using Voronoi grids, Geoscientific Model Development, 11, 3747–3780, https://doi.org/10.5194/gmd-11-3747-2018, https://www.geosci-model-dev.net/11/3747/2018/, 2018.

Hulbe, C.: Is ice sheet collapse in West Antarctica unstoppable?, Science, 356, 910–911, 2017.

Hutter, K.: Theoretical glaciology, Reidel Publ., Dordrecht, Netherlands, https://doi.org/10.1007/978-94-015-1167-4, 1983.

Jenkins, A., Dutrieux, P., Jacobs, S., Steig, E. J., Gudmundsson, G. H., Smith, J., and Heywood, K. J.: Decadal ocean forcing and Antarctic ice sheet response: Lessons from the Amundsen Sea, Oceanography, 29, 106–117, 2016.

Joughin, I., Smith, B. E., and Medley, B.: Marine ice sheet collapse potentially under way for the Thwaites Glacier Basin, West Antarctica, Science, 344, 735–738, 2014.

Konrad, H., Shepherd, A., Gilbert, L., Hogg, A. E., McMillan, M., Muir, A., and Slater, T.: Net retreat of Antarctic glacier grounding lines, Nature Geoscience, 11, 258, 2018.

Li, D., Gurnis, M., and Stadler, G.: Towards adjoint-based inversion of time-dependent mantle convection with nonlinear viscosity, Geophysical Journal International, 209, 86–105, https://doi.org/10.1093/gji/ggw493, https://doi.org/10.1093/gji/ggw493, 2017.

Liefferinge, B. V. and Pattyn, F.: Using ice-flow models to evaluate potential sites of million year-old ice in Antarctica, Climate of the Past, 9, 2335–2345, 2013.

MacAyeal, D. R.: Ice-shelf backpressure: form drag versus dynamic drag, in: Dynamics of the West Antarctic Ice Sheet, edited by Van Der Veen, C. J. and Oerlemans, J., p. 141, D. Reidel Publishing Company, Dordrecht, Holland, 1987.

Mercer, J. H.: West Antarctic ice sheet and CO2 greenhouse effect: a threat of disaster, Nature, 271, 321, 1978.

Morland, L.: Unconfined ice-shelf flow, in: Dynamics of the West Antarctic Ice Sheet, pp. 99–116, Springer, 1987.

Pegler, S. S. and Worster, M. G.: Dynamics of a viscous layer flowing radially over an inviscid ocean, Journal of Fluid Mechanics, 696, 152–174, 2012.

Perego, M., Gunzburger, M., and Burkardt, J.: Parallel finite-element implementation for higher-order ice-sheet models, Journal of Glaciology, 58, 76–88, https://doi.org/10.3189/2012JoG11J063, 2012.

Perego, M., Price, S., and Stadler, G.: Optimal initial conditions for coupling ice sheet models to Earth system models, Journal of Geophysical Research: Earth Surface, 119, 1894–1917, 2014.

Phipps, E. and Pawlowski, R.: Efficient Expression Templates for Operator Overloading-Based Automatic Differentiation, in: Recent Advances in Algorithmic Differentiation, edited by Forth, S., Hovland, P., Phipps, E., Utke, J., and Walther, A., vol. 87 of *Lecture Notes in Computational Science and Engineering*, pp. 309–319, Springer, Berlin, https://doi.org/10.1007/978-3-642-30023-3_28, 2012.

Reese, R., Gudmundsson, G. H., Levermann, A., and Winkelmann, R.: The far reach of ice-shelf thinning in Antarctica, Nature Climate Change, 8, 53, 2018.

Rignot, E., Mouginot, J., and Scheuchl, B.: Ice flow of the antarctic ice sheet, Science, 333, 1427–1430, https://doi.org/10.1126/science.1208336, 2011.

Rignot, E., Mouginot, J., Morlighem, M., Seroussi, H., and Scheuchl, B.: Widespread, rapid grounding line retreat of Pine Island, Thwaites, Smith, and Kohler glaciers, West Antarctica, from 1992 to 2011, Geophysical Research Letters, 41, 3502–3509, 2014.

Royston, S. and Gudmundsson, G. H.: Changes in ice-shelf buttressing following the collapse of Larsen A Ice Shelf, Antarctica, and the resulting impact on tributaries, Journal of Glaciology, 62, 905–911, 2016.

Schoof, C.: Ice sheet grounding line dynamics: Steady states, stability, and hysteresis, Journal of Geophysical Research: Earth Surface, 112, 2007.

Schoof, C.: Marine ice sheet stability, Journal of Fluid Mechanics, 698, 62–72, 2012.

Seroussi, H., Morlighem, M., Larour, E., Rignot, E., and Khazendar, A.: Hydrostatic grounding line parameterization in ice sheet models, The Cryosphere, 8, 2075–2087, 2014.

Seroussi, H., Nowicki, S., Simon, E., Abe-Ouchi, A., Albrecht, T., Brondex, J., Cornford, S., Dumas, C., Gillet-Chaulet, F., Goelzer, H., Golledge, N. R., Gregory, J. M., Greve, R., Hoffman, M. J., Humbert, A., Huybrechts, P., Kleiner, T., Larour, E., Leguy, G., Lipscomb, W. H., Lowry, D., Mengel, M., Morlighem, M., Pattyn, F., Payne, A. J., Pollard, D., Price, S. F., Quiquet, A., Reerink, T. J., Reese, R., Rodehacke, C. B., Schlegel, N.-J., Shepherd, A., Sun, S., Sutter, J., Van Breedam, J., van de Wal, R. S. W., Winkelmann, R., and Zhang, T.: initMIP-Antarctica: an ice sheet model initialization experiment of ISMIP6, The Cryosphere, 13, 1441–1471, https://doi.org/10.5194/tc-13-1441-2019, https://www.the-cryosphere.net/13/1441/2019/, 2019.

Tezaur, I. K., Perego, M., Salinger, A. G., Tuminaro, R. S., and Price, S.: Albany/FELIX: a parallel, scalable and robust, finite element, first-order Stokes approximation ice sheet solver built for advanced analysis, Geoscientific Model Development, 8, 1–24, https://doi.org/10.5194/gmd-8-1-2015, 2015a.

Tezaur, I. K., Tuminaro, R. S., Perego, M., Salinger, A. G., and Price, S. F.: On the scalability of the Albany/FELIX first-order Stokes approximation ice sheet solver for large-scale simulations of the Greenland and Antarctic ice sheets, Procedia Computer Science, 51, 2026–2035, 2015b.

Thomas, R. H.: The dynamics of marine ice sheets, The Journal of Glaciology, 24, 167–178, 1979.

Thomas, R. H. and MacAyeal, D. R.: Derived Characteristics of the Ross Ice Shelf, Antarctica, Journal of Glaciology, 28, 397–412, https://doi.org/10.3189/s0022143000005025, 1982.

Van Der Veen, C. J.: Fundamentals of Glacier Dynamics, CRC Press, Boca Raton, FL, 2 edn., 2013.

Wearing, M.: The Flow Dynamics and Buttressing of Ice Shelves, Ph.D. thesis, University of Cambridge, 2016.

Supplementary Material to "Diagnosing the sensitivity of grounding line flux to changes in sub-ice shelf melting"

Correlations between N_r and various metrics

While the main goal of the study was to investigate the ability of the buttressing number (N_b) to predict the GLF response number (N_r), we also assessed the predictive skill of a range of other metrics. This was motivated by the lack of a clear theoretical justification for expecting N_b to predict N_r and a concern that observed correlations may be spurious. To this end, we calculated correlation coefficients for a variety of locally defined metrics related to the stress state of the ice shelf (Table S01). Correlations for each metric were calculated for the MISMIP+ and Larsen C domains and in both cases, the calculations were made with and without filtering points by the shear metric, m_s (Eq. (**??**)).

The first set of metrics are the buttressing number (N_b) defined for a number of different normal directions, as discussed in the main paper. We also considered normal directions rotated 30° and 45° from the $\mathbf{n}_{p1}$ direction, which was motivated by the observation in Figs. 5a and S6, respectively, of maximum correlations in those directions. Additionally, we included the shear metric, m_s, and the quantity "backstress" (Thomas, 1979; Thomas and MacAyeal, 1982; MacAyeal, 1987), which as described in Appendix B is equivalent to $N_b(\mathbf{n}_f)N_0$. For completeness, we also assess the principal stresses, the maximum shear stress, and the stress in the flow direction. Finally, we include the equivalent ocean pressure, N_0 (which is proportional to ice thickness), and the two terms of the force balance used to calculate backstress.

There is not a single metric that has the highest correlation across all four cases. The metrics that perform the best across all cases are backstress (B_s) and the buttressing number (N_b) using normal directions between the $\mathbf{n}_{p1}$ and $\mathbf{n}_{p2}$ directions. In general, $N_b(\mathbf{n}_{p1})$ does not perform particularly well, reiterating the conclusions in the main paper that it cannot be recommended as a reliable predictor of changes in flux across the grounding line. Also of note are what appear to be spurious correlations. For example, the driving force, F_D, and the ocean backpressure, N_0, generate the largest correlation coefficients for the MISMIP+ case limited to points where $m_s < 1$, but have no particular skill when all points are considered. Similarly, the longitudinal stretching force (F_L) for the MISMIP+ with $m_s < 1$ has high skill, but yields correlation coefficients close to 0 for the other cases. There is no theoretical reason to expect any of these metrics to relate directly to change in flux across the grounding line. These examples highlight the need for caution in extrapolating what appear to be strong correlations but are based on the analysis of a specific ice shelf configuration.

The conclusion of this detailed correlation analysis confirms that of the other analyses in the paper: no single metric can be identified that can be used with confidence to predict N_r in general. While high correlations can be found in specific circumstances, there is not a single metric with universal skill in predictability, and applications to the real-world ice shelf fail to provide any relationships with practical utility.

		MISMIP+		Larsen C	
		m_s<1	All m_s	m_s<1	All m_s
	# points:	309	404	6192	8814
Variable	Description				
$N_b(\mathbf{n}_{p1})$	Eq. 10	0.90	0.54	0.49	0.38
$N_b(\mathbf{n}_{p2})$	Eq. 10	0.58	0.66	0.31	0.45
$N_b(\mathbf{n}_{p1}+30°)$	Eq. 10, Fig. 5a	0.94	0.86	0.50	0.50
$N_b(\mathbf{n}_{p1}+45°)$	Eq. 10, Fig. S8	0.87	0.87	0.47	0.53
$N_b(\mathbf{n}_f)$	Eq. 10	0.71	0.78	0.45	0.43
B_s	Eq. B9	0.92	0.83	0.60	0.55
m_s	Eq. 13	0.40	0.66	0.06	0.10
σ_1	1st princ. stress	0.64	0.37	0.24	0.31
σ_2	2nd princ. stress	0.46	0.63	0.23	0.51
τ_{max}	Max. shear stress	0.30	0.55	0.04	0.44
σ_{flow}	stress in flow dir.	0.17	0.42	0.28	0.41
N_0,H	Eq. A8	0.96	0.60	0.54	0.39
F_D	Eq. B2	0.97	0.61	0.59	0.46
F_L	Eq. B3	0.84	0.00	0.03	0.25

Table S01. Correlation coefficients (r) between various metrics and N_{rp} calculated for the MISMIP+ and Larsen C model domains. For each domain, r values are reported for two situations: 1) where the shear metric m_s is less than 1, and 2) for all values of m_s. In both situations, grid cells intersecting the grounding line and grid cells adjacent to those points are excluded. Also, for both situations applied to the MISMIP+ domain, points on the ice shelf east of $x = 480$ km are excluded. Values lower than the 50th percentile are shown with a white background, and values between the 50th and 99th percentile are shown with increasingly dark green shading.

~~Histograms showing the angular difference between $\mathbf{n}_{p1}$ and $\mathbf{n}_f$. Points analyzed are those from Fig. 4.~~

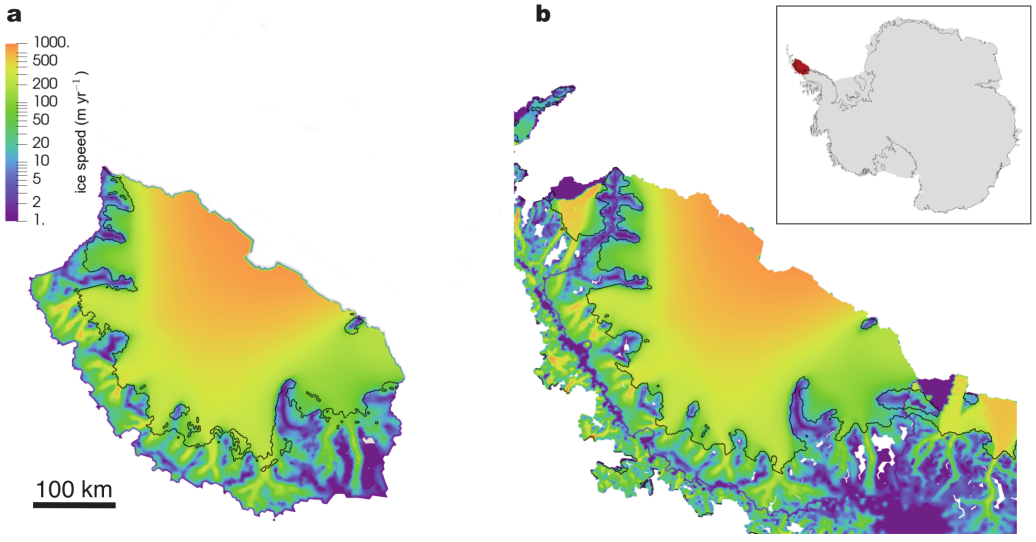

Figure S1. The modeled (a) and observed (b) surface ice speed for Larsen C Ice Shelf. Note that after 100 yr relaxation, the grounding line position in the modeled result is different from present-day observation.

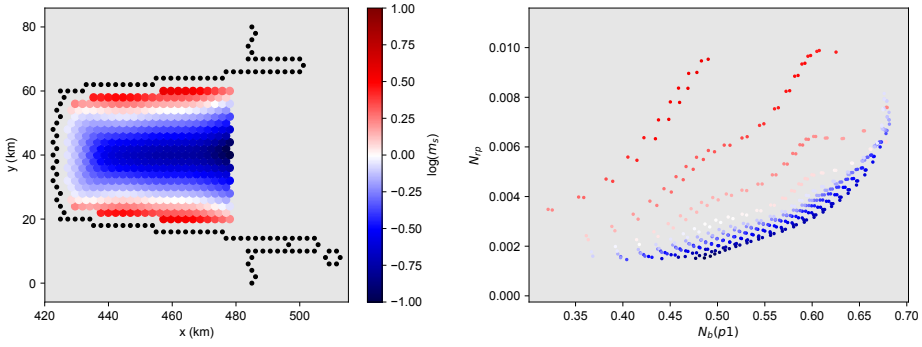

Figure S2. Shear ratio metric, m_s. a) Map of $\log(m_s)$. Positive values correspond to $m_s > 1$ where the maximum shear stress is large relative to the average normal stress, while negative values correspond to $m_s < 1$. Black dots indicate grounding line location. b) Plot of $N_b(p1)$ versus n_{rp} colored by m_s as in a).

~~Histograms for the maximum (red) and minimum (blue) percent speed increases in grid cells adjacent to a thickness perturbation on the Larsen C ice shelf, plotted as a function of angular distance with respect to $\mathbf{n}_{p1}$ (a) and $\mathbf{n}_f$ (b).~~

~~An example of the local change (ratio, in %) in the ice thickness gradient in x (a), ice thickness gradient in y (b), ice speed (c), ice velocity (d), principal strain rates (e, f), and buttressing number (g, h) following a local perturbation to the ice shelf thickness. In e) and g), changes (colors) are associated with the $\mathbf{n}_{p1}$ direction (white-dashed line) and for f) and h) changes~~

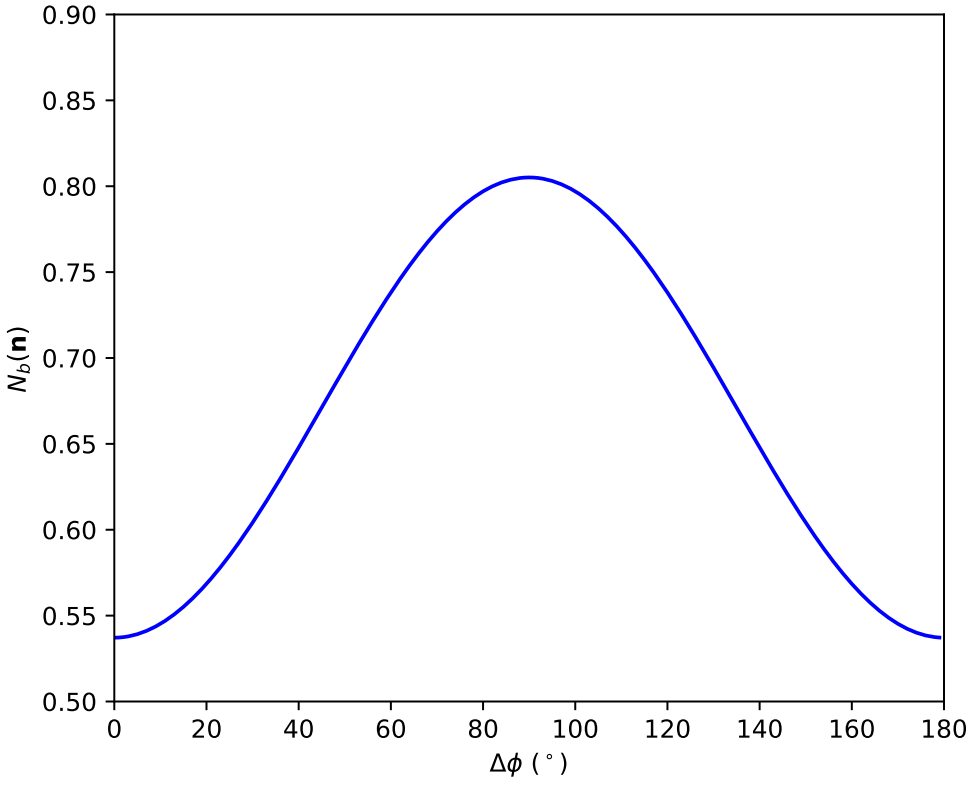

Figure S3. N_b values when $\mathbf{n}$ is rotated counterclockwise by $\Delta\phi$ degrees relative to the direction corresponding to σ_{p1} ($\mathbf{n}_{p1}$).

~~are associated with the $\mathbf{n}_{p2}$ direction (black-dashed line). The inset in (b) is a zoom-in of the velocity change around the perturbation. The small panel on the right shows the location of the perturbation.~~

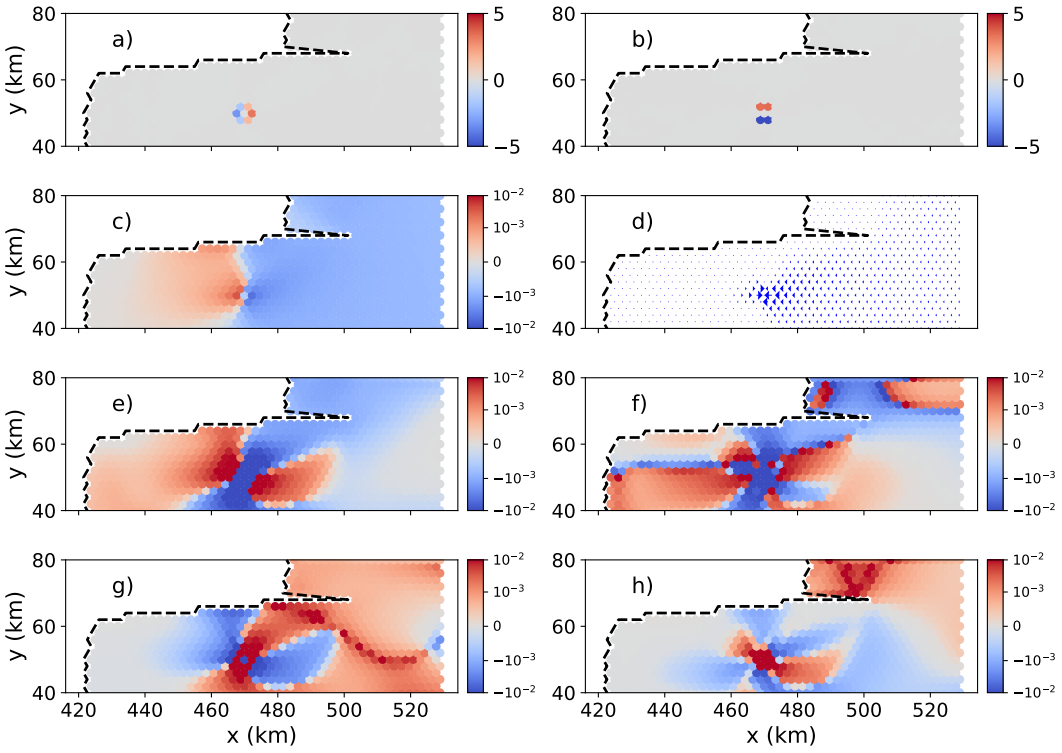

Figure S4. An example of the local change (ratio, in %) in the ice thickness gradient in x (a), ice thickness gradient in y (b), ice speed (c), ice velocity (d), principal strain rates (e, f), and buttressing number (g, h) following a local perturbation to the ice shelf thickness. In e) and g), changes (colors) are associated with the $\mathbf{n}_{p1}$ direction ~~(white-dashed line)~~ and for f) and h) changes are associated with the $\mathbf{n}_{p2}$ direction~~(black-dashed line). The inset in (b) is a zoom-in of the velocity change around the perturbation~~.

~~Correlation between the change in normal stress and the change in ice surface speed along grounding line (i.e., Υ_{gl} from Eq. (13)) for Larsen C experiments. The horizontal axis shows how Υ_{gl} varies as a function of the direction $\mathbf{n}$ used to define the normal stress, rotated counterclockwise from $\mathbf{n}_{p1}$. The blue shaded area is the range for all perturbation experiments (same as in Fig. 5a) and the thick black curve is their mean value.~~

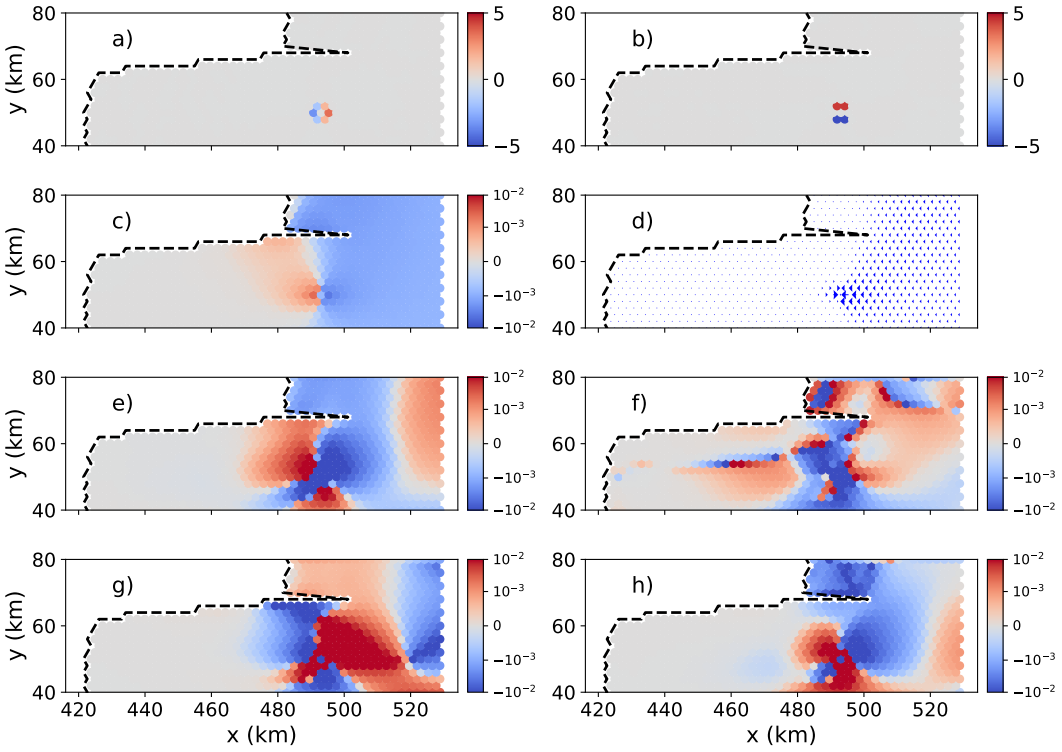

Figure S5. An example of the local change (ratio, in %) in the ice thickness gradient in x (a), ice thickness gradient in y (b), ice speed (c), ice velocity (d), principal strain rates (e, f), and buttressing number (g, h) following a local perturbation to the ice shelf thickness. In e) and g), changes (colors) are associated with the $\mathbf{n}_{p1}$ direction ~~(white-dashed line)~~ and for f) and h) changes are associated with the $\mathbf{n}_{p2}$ direction~~(black-dashed line)~~. ~~The inset in (b) is a zoom-in of the velocity change around the perturbation.~~

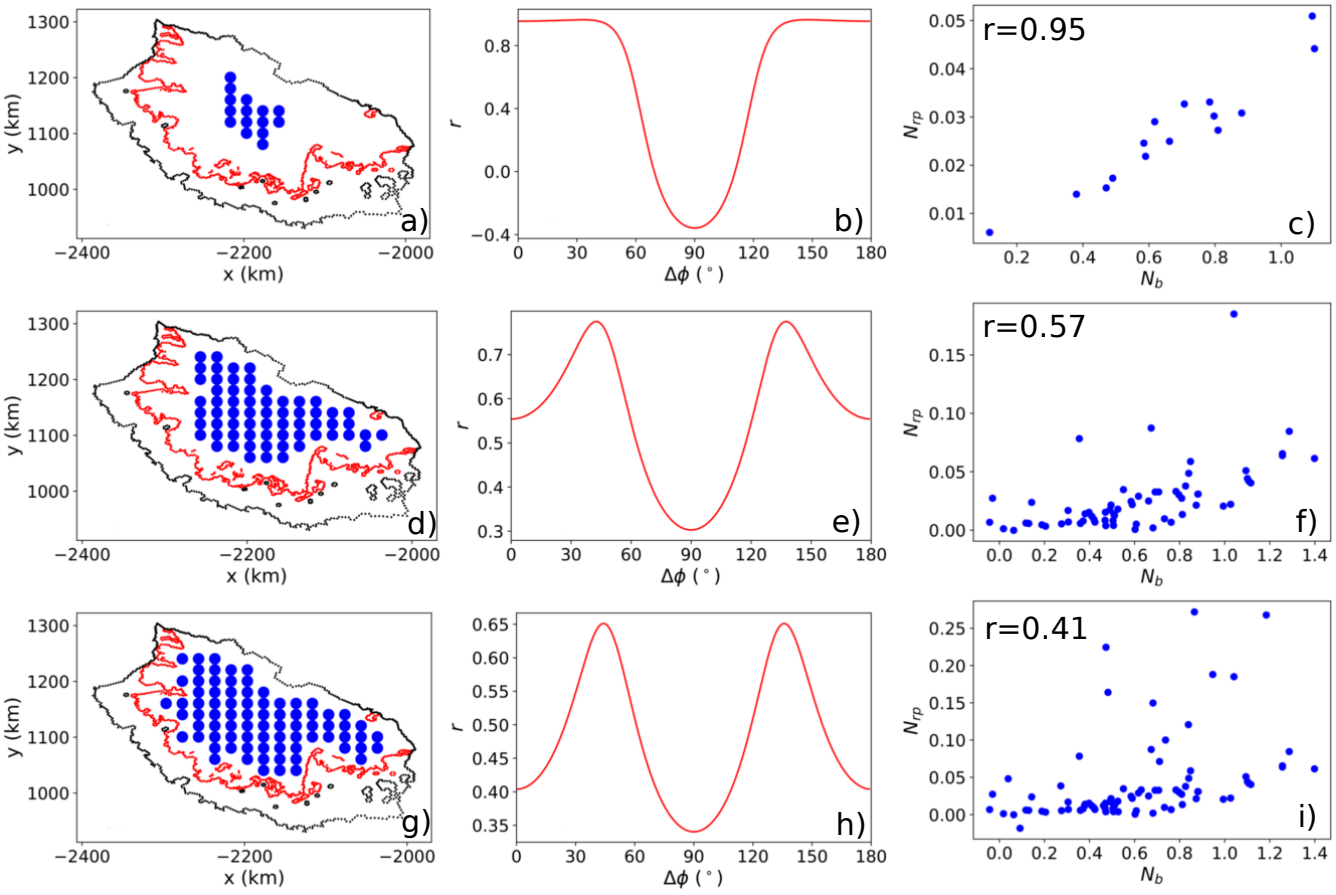

Figure S6. (a, d, g) The ~~change in buttressing number ΔN_b at~~ locations of the ~~neighboring cells with maximum ice speed increase for each~~ 20 km × 20 km perturbation ~~point in the inset of Fig~~boxes (solid blue dots). ~~12 that are > 50 km away from~~ The red and black dotted lines represent the grounding line and the ~~calving front~~ boundary of ~~the Larsen C shelf~~model domain, respectively. ~~Changes in buttressing are calculated along the direction $\Delta\phi$~~(b, e, h) The N_{rp} : N_b correlation coefficients for each direction rotated counterclockwise ~~relative to~~ from the ~~$\mathbf{n}_{p1}$~~ direction of $\mathbf{n}_{p1}$. (c, f, i) The corresponding scatter plots for $N_b(\mathbf{n_{p1}})$ and N_{rp}.